

Improved Convergence Rates of Windowed Anderson Acceleration for Symmetric Fixed-Point Iterations

Casey Garner* Gilad Lerman* Teng Zhang†

March 11, 2024

Abstract

This paper studies the commonly utilized windowed Anderson acceleration (AA) algorithm for fixed-point methods, $x^{(k+1)} = q(x^{(k)})$. It provides the first proof that when the operator q is linear and symmetric the windowed AA, which uses a sliding window of prior iterates, improves the root-linear convergence factor over the fixed-point iterations. When q is nonlinear, yet has a symmetric Jacobian at a fixed point, a slightly modified AA algorithm is proved to have an analogous root-linear convergence factor improvement over fixed-point iterations. Simulations verify our observations. Furthermore, experiments with different data models demonstrate AA is significantly superior to the standard fixed-point methods for Tyler’s M-estimation.

Keywords: Anderson acceleration, fixed-point method, Tyler’s M-estimation

MSC codes: 65F10, 65H10, 68W40

1 Introduction

This paper investigates the convergence properties of the popular acceleration technique for fixed-point problems called Anderson acceleration (AA). The method, originally introduced by D.G. Anderson in the context of integral equations (1965), utilizes a history of prior iterates to accelerate the classical fixed-point iteration, aka the Picard iteration (Picard, 1890). A brief history of the method, including its relationship to Pulay mixing, nonlinear GMRES, and quasi-Newton methods, can be found in the literature (Fang and Saad, 2009; Kelley, 2018; Potra and Engler, 2013; Pulay, 1980). A renewed interest in AA came about following the work of Walker and Ni (2011) where they demonstrated the effectiveness of AA in numerous applications such as nonnegative matrix

*School of Mathematics, University of Minnesota (garne214@umn.edu, lerman@umn.edu)

†Department of Mathematics, University of Central Florida (Teng.Zhang@ucf.edu)

factorization and domain decomposition. Recently, AA, in various forms, has been studied in a myriad of settings and applied in numerous applications, see, for example, (Geist and Scherrer, 2018; Shi et al., 2019; Sun et al., 2021; Zhang et al., 2016; Brezinski et al., 2019; Bian et al., 2021, 2022).

Despite a long history of use and strong recent interest, the accelerated convergence of AA is still not completely understood. The first mathematical convergence results for AA, for linear and nonlinear problems, were established by Toth and Kelley (2015); however, they only proved AA did not worsen the convergence of the fixed-point iteration. Their theory did not prove AA converged faster than the fixed-point method, as often witnessed in practice. Following Toth and Kelley, further efforts have shed more light on the convergence behavior of AA. In the papers by Evans et al. (2020), Pollock et al. (2019), and Pollock and Rebholz (2021), they proved AA improved convergence by studying the “stage- k gain” of AA, which shows how much AA improves upon the fixed-point method at iteration k . Their analysis showed AA can best the fixed-point iteration by a factor $0 \leq \theta_k \leq 1$ known as the gain at step k ; however, as noted by De Sterck and He, “it is not clear how θ_k may be evaluated or bounded in practice or how it may translate to an improved linear asymptotic convergence factor” (2022). In De Sterck and He (2022), they note some intriguing properties of AA, such as how the linear asymptotic convergence factor depends on the initialization of the method. De Sterck, He, and Krzysik continuing this study related windowed AA to Krylov methods and developed new results on residual convergence bounds for linear fixed-point iterations (2024); however, they note in their conclusion that bounding the asymptotic convergence factors remains an open and difficult question. In a different direction, Rebholz and Xiao (2023) proved how AA affects the convergence rate of superlinearly and sublinearly converging fixed-point iterations.

The aforementioned papers have added much to our understanding of the convergence of AA in the past decade, and this paper joins the conversation by establishing the improved root-linear convergence factor of AA over the fixed-point iteration. To the best of our knowledge, this paper is the first to answer this open question and present a bound which clearly shows AA has a better asymptotic convergence factor than the fixed-point iteration. Notably, our approach to proving the claim is novel and does not utilize the notation of gain as defined in prior works, see (Evans et al., 2020; Pollock et al., 2019; Pollock and Rebholz, 2021). Furthermore, our results only require common assumptions found in the literature. For example, we assume the Jacobian matrix of the operator \mathbf{q} , for which we desire to compute fixed points, is symmetric at fixed points (Scieur, 2019; Scieur et al., 2016).

It is worth noting that positive asymptotic convergence results have been proven for other variants of AA. Recently, De Sterck et al. (2024) appeared and presented a characterization of the convergence for a restarted version of AA. Their results fully describe the behavior of a restarted AA iteration

for solving 2×2 linear systems. This paper contains similar results to an earlier work, Both et al. (2019), where the authors proved a restarted version of AA has a better asymptotic convergence factor compared to the fixed-point method. Our work differs substantially because we do not study a restarted AA method but a windowed AA method, which uses a sliding window of prior iterates to compute the next iterate. We compare different AA variants in Section 4.3.

Definitions and notation: $\mathbb{R}^{n \times n}$ and $\mathcal{S}^{n \times n}$ denote the set of real n -by- n and real symmetric n -by- n matrices respectively. Given $\mathbf{A} \in \mathbb{R}^{n \times n}$, its ℓ_2 norm (or spectral/operator norm) is denoted $\|\mathbf{A}\|$. The largest and the smallest eigenvalues of a matrix \mathbf{A} are denoted $\lambda_{\max}(\mathbf{A})$ and $\lambda_{\min}(\mathbf{A})$ respectively. Given the vector $\mathbf{x} \in \mathbb{R}^n$, $\text{Diag}(\mathbf{x})$ denotes the diagonal matrix formed by \mathbf{x} . For any three points $O, P, Q \in \mathbb{R}^n$, $\angle(OPQ) \in [0, \pi]$ represents the angle between the vectors \vec{PO} and \vec{PQ} . For any sequence $\{\mathbf{x}^{(k)}\}$ that converges to \mathbf{x}_* , we define its r -linear convergence factor to be

$$\rho_{\{\mathbf{x}^{(k)}\}} = \limsup_{k \rightarrow \infty} \|\mathbf{x}_* - \mathbf{x}^{(k)}\|^{\frac{1}{k}}.$$

Then, we say $\{\mathbf{x}^{(k)}\}$ converges r -linearly with r -linear convergence factor $\rho_{\{\mathbf{x}^{(k)}\}}$, and here the prefix “ r -” stands for “root”.

Organization of the rest of the paper: Section 2 introduces the problem setting and defines the AA algorithm we study; Section 3 states the main results of the paper with the key result being a proven upper bound on the root-linear convergence factor for AA when the Jacobian matrix is symmetric; Section 4 presents numerical experiments for both linear and nonlinear operators and compares the performance of different types of AA variants; Section 5 contains the proofs of our results; the paper concludes in Section 6 with directions for future inquiry.

2 Anderson Acceleration

This paper concerns the convergence of acceleration methods for computing fixed points of an operator $\mathbf{q} : \mathbb{R}^n \rightarrow \mathbb{R}^n$, i.e, computing points $\mathbf{x}_* \in \mathbb{R}^n$ such that $\mathbf{x}_* = \mathbf{q}(\mathbf{x}_*)$. For this problem, the standard fixed-point iteration/method is the iterative procedure described by

$$\mathbf{x}^{(k+1)} = \mathbf{q}(\mathbf{x}^{(k)}). \tag{1}$$

In this work, we study the windowed AA algorithm with depth m , AA(m), applied to the fixed-point iteration (1). A full description of AA(m) is given in Algorithm 1. The key idea behind the method is to use a history of at most $m + 1$ points to construct the next update at each iteration. A linear least-squares problem, (2), is solved at each iteration to determine how to utilize the prior iterates to form the next update. It is worth noting that any vector norm can be utilized in (2) without changing the convergence theory for AA. As discussed in Section 1, AA has proven very

effective in many applications and this practical utility has motivated the resurgence of convergence analysis for the method.

Algorithm 1 Windowed Anderson acceleration algorithm of depth m ; AA(m)

Input: Operator $\mathbf{q} : \mathbb{R}^n \rightarrow \mathbb{R}^n$, initialization $\mathbf{x}^{(0)} \in \mathbb{R}^n$, depth $m \in \{1, 2, \dots\}$

Output: An estimation of the fixed point of \mathbf{q} .

Steps:

1: $\mathbf{x}^{(1)} = \mathbf{q}(\mathbf{x}^{(0)})$.

2: For $k \geq 1$, let $m_k = \min(m, k)$. Solve the minimization problem

$$\min_{\sum_{j=k-m_k}^k \alpha_j^{(k)} = 1} \left\| \sum_{j=k-m_k}^k \alpha_j^{(k)} (\mathbf{q}(\mathbf{x}^{(j)}) - \mathbf{x}^{(j)}) \right\|, \quad (2)$$

and let

$$\mathbf{x}^{(k+1)} = \sum_{j=k-m_k}^k \alpha_j^{(k)} \mathbf{q}(\mathbf{x}^{(j)}).$$

3: Repeat Step 2 for $k \geq 2$. An estimation of the fixed point is given by $\lim_{k \rightarrow \infty} \mathbf{x}^{(k)}$.

3 Main Results

This section presents our main results showcasing AA(m) has an improved r -linear convergence factor over the fixed-point iteration. Section 3.1 shows in the case of linear and symmetric operators AA(m) converges faster than the fixed-point iteration with the convergence rate given in Theorem 1. It also clarifies some geometric ideas of the proof, though the intricate geometric estimates are left to Section 5. Another idea that makes the proofs more elegant is a reformulation of AA(m) and Section 3.2 describes it. Section 3.3 shows when \mathbf{q} is nonlinear, yet has a symmetric Jacobian at the solution, a modified version of Algorithm 1 has an analogous root-linear convergence factor improvement over the fixed-point iteration when initialized near a solution. Section 3.4 closes with additional remarks and discussion concerning our results.

3.1 Linear Symmetric Operators

We begin with the convergence rate of AA(m) for linear symmetric operators \mathbf{q} , where $\mathbf{q}(\mathbf{x}) = \mathbf{W}\mathbf{x} + \mathbf{a}$ with $\mathbf{W} \in \mathcal{S}^{n \times n}$ and $-1 < \lambda_{\min}(\mathbf{W}) \leq \lambda_{\max}(\mathbf{W}) < 1$. Theorem 1 establishes the convergence rate of AA(m) over every two iterations based on $\lambda_{\min}(\mathbf{W})$ and $\lambda_{\max}(\mathbf{W})$ to provide

an upper bound on the r -linear convergence factor of AA(m).

Theorem 1 (Convergence factor of AA(m) for linear symmetric operators). *Let $\mathbf{q}(\mathbf{x}) = \mathbf{W}\mathbf{x} + \mathbf{a}$ with $\mathbf{W} \in \mathcal{S}^{n \times n}$ and $\|\mathbf{W}\| < 1$. Then AA(m) converges r -linearly to a fixed point of \mathbf{q} with rate bounded by $\sqrt{w_0\|\mathbf{W}\|}$ for any initialization, where*

$$w_0 = \sup_{a \geq 0} \sin \left[\sin^{-1} \left(\frac{|\lambda_{\max}(\mathbf{W}) - \lambda_{\min}(\mathbf{W})|a}{\sqrt{4 + (2 - \lambda_{\max}(\mathbf{W}) - \lambda_{\min}(\mathbf{W}))^2 a^2}} \right) + \left| \tan^{-1}(a) - \tan^{-1} \left(\left(1 - \frac{\lambda_{\max}(\mathbf{W}) + \lambda_{\min}(\mathbf{W})}{2}\right)a \right) \right| \right]. \quad (3)$$

More specifically, if $\{\mathbf{x}^{(k)}\}$ is the sequence generated by AA(m), then for all $k \geq 2$

$$\frac{\|(\mathbf{W} - \mathbf{I})(\mathbf{x}^{(k+1)} - \mathbf{x}_*)\|}{\|(\mathbf{W} - \mathbf{I})(\mathbf{x}^{(k-1)} - \mathbf{x}_*)\|} \leq w_0 \|\mathbf{W}\|, \quad (4)$$

and w_0 is bounded by $\|\mathbf{W}\|$ with $w_0 = \|\mathbf{W}\|$ if and only if $\lambda_{\max}(\mathbf{W}) = -\lambda_{\min}(\mathbf{W})$.

To begin understanding this result, we provide a geometric interpretation of w_0 . While the expression in (3) is rather complicated, it actually follows from a geometric problem. Assume P is an arbitrary point in the xy -plane with y -coordinate equal to 1 and Q is a point on the circle centered at $C = (0, \frac{\lambda_{\max}(\mathbf{W}) + \lambda_{\min}(\mathbf{W})}{2})$ with radius $\frac{\lambda_{\max}(\mathbf{W}) - \lambda_{\min}(\mathbf{W})}{2}$. Let O be the origin, then w_0 is an upper bound on the largest possible $\sin \angle(OPQ)$ formed as P traverses along the line $y = 1$ and Q traverses along the circle. A visualization of this set-up is given in Figure 1. To understand how this geometric object relates to (3), we first note

$$\angle(OPQ) \leq \angle(CPQ) + \angle(OPC). \quad (5)$$

Let $R = (0, 1)$ and assume $|PR| = 1/a$, then

$$\sin \angle(CPQ) \leq \frac{|QC|}{|CP|} = \frac{|\lambda_{\max}(\mathbf{W}) - \lambda_{\min}(\mathbf{W})|a}{\sqrt{4 + (2 - \lambda_{\max}(\mathbf{W}) - \lambda_{\min}(\mathbf{W}))^2 a^2}}. \quad (6)$$

In addition,

$$\begin{aligned} \angle(OPC) &= |\angle(OPR) - \angle(CPR)| = \left| \tan^{-1} \frac{|OR|}{|PR|} - \tan^{-1} \frac{|CR|}{|PR|} \right| \\ &= \left| \tan^{-1}(a) - \tan^{-1} \left(\left(1 - \frac{\lambda_{\max}(\mathbf{W}) + \lambda_{\min}(\mathbf{W})}{2}\right)a \right) \right|. \end{aligned}$$

Combining these inequalities we have

$$\begin{aligned} \angle(OPQ) &\leq \sin^{-1} \left(\frac{|\lambda_{\max}(\mathbf{W}) - \lambda_{\min}(\mathbf{W})|a}{\sqrt{4 + (2 - \lambda_{\max}(\mathbf{W}) - \lambda_{\min}(\mathbf{W}))^2 a^2}} \right) \\ &\quad + \left| \tan^{-1}(a) - \tan^{-1} \left(\left(1 - \frac{\lambda_{\max}(\mathbf{W}) + \lambda_{\min}(\mathbf{W})}{2}\right)a \right) \right|. \end{aligned}$$

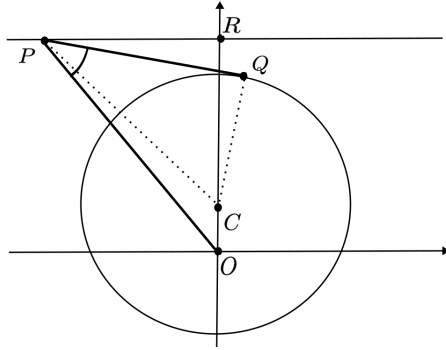


Figure 1: Visualization of w_0 defined in (3). It represents the sine of the largest possible angle $\angle(OPQ)$ formed as P traverses along the line $y = 1$ and Q traverses along the circle.

Furthermore, for any a and its associated P , we could choose Q such that this upper bound is obtained by making (5) and (6) tight. In particular, Q is chosen such that \vec{PQ} is tangent to the circle, making $\angle(PQC) = \pi/2$ and (6) hold with equality, and \vec{PC} is contained inside the cone defined by \vec{PO} and \vec{PQ} , as visualized in Figure 1. As a result, w_0 is the largest possible value of $\sin \angle(OPQ)$.

The following proposition shows the improvement ratio (4) in Theorem 1 is an equality in the special case where \mathbf{W} is scalar matrix.

Proposition 2 (A special case of a tight bound). *If \mathbf{W} is a scalar matrix and $AA(1)$ is initialized in a particular fashion, with \mathbf{x}_0 and \mathbf{x}_1 independently initialized, then (4) is an equality and $w_0 = \|\mathbf{W}\|/\sqrt{2 - \|\mathbf{W}\|}$.*

Theorem 1 implies that the r -linear convergence factor of $AA(m)$ is at most $\|\mathbf{W}\|$, which is the r -linear convergence factor of the fixed-point iteration. The theorem also implies provided $\lambda_{\max}(\mathbf{W}) \neq -\lambda_{\min}(\mathbf{W})$ the convergence factor is strictly smaller. We extend this result by showing if $m \geq 2$ the convergence factor of $AA(m)$ is always strictly better than the rate of the fixed-point method.

Proposition 3 (Improved r -linear convergence factor). *If either $m \geq 2$ or $\lambda_{\max}(\mathbf{W}) \neq -\lambda_{\min}(\mathbf{W})$, then the r -linear convergence factor of $AA(m)$ is strictly smaller than $\|\mathbf{W}\|$, which is the r -linear convergence factor of the fixed-point iteration. If on the other hand $m = 1$ and $\lambda_{\max}(\mathbf{W}) = -\lambda_{\min}(\mathbf{W})$, then the convergence factor of $AA(m)$ may be $\|\mathbf{W}\|$.*

3.2 A Helpful Reformulation of Anderson Acceleration

The proofs of the above results require intricate geometric estimates. Nevertheless, they become simpler by the following reformulation of $AA(m)$. To present our equivalent reformula-

tion of AA(m), we may assume without loss of generality $\mathbf{a} = \mathbf{0}$ and as a result $\mathbf{x}_* = \mathbf{0}$. Let $\tilde{\mathbf{x}}^{(k)} = \mathbf{q}(\mathbf{x}^{(k)}) - \mathbf{x}^{(k)}$, then AA(m) updates $\tilde{\mathbf{x}}$ iteratively as follows:

1. Let $\tilde{\mathbf{y}}^{(k+1)}$ be the point on the affine subspace spanned by $\tilde{\mathbf{x}}^{(k-m_k)}, \dots, \tilde{\mathbf{x}}^{(k)}$ with the smallest norm, $\|\tilde{\mathbf{y}}^{(k+1)}\|^2$.
2. $\tilde{\mathbf{x}}^{(k+1)} = \mathbf{q}(\tilde{\mathbf{y}}^{(k+1)})$.

The equivalency of the first step of the reformulated procedure follows from the definition of AA(m). By the definition of $\alpha_j^{(k)}$, we have

$$\tilde{\mathbf{y}}^{(k+1)} = \sum_{j=k-m_k}^k \alpha_j^{(k)} \tilde{\mathbf{x}}^{(j)} = \sum_{j=k-m_k}^k \alpha_j^{(k)} (\mathbf{q}(\mathbf{x}^{(j)}) - \mathbf{x}^{(j)}).$$

The equivalency of the second is derived as follows:

$$\tilde{\mathbf{x}}^{(k+1)} = (\mathbf{q} - \mathbf{I})\mathbf{x}^{(k+1)} = (\mathbf{q} - \mathbf{I})\left(\sum_{j=k-m_k}^k \alpha_j^{(k)} \mathbf{q}(\mathbf{x}^{(j)})\right) = \mathbf{q}\left(\sum_{j=k-m_k}^k \alpha_j^{(k)} (\mathbf{q} - \mathbf{I})\mathbf{x}^{(j)}\right) = \mathbf{q}(\tilde{\mathbf{y}}^{(k+1)}),$$

where we use the fact $\mathbf{q}(\mathbf{x}) = \mathbf{W}\mathbf{x}$. The compactness of this reformulation removes the discussion of the coefficients, $\alpha_j^{(k)}$, which often occurs in discussions of AA. Thus, with this reformulation we do not need to discuss the boundedness of the coefficients directly in the linear setting. Additionally, this simplification aids the geometric arguments we present which are similar in nature to the discussion provided in Section 3.1.

3.3 Nonlinear Operator

Moving beyond linear operators, we now assume \mathbf{q} is nonlinear and has a first-order Taylor expansion at the fixed point \mathbf{x}_* with symmetric Jacobian $\nabla\mathbf{q}(\mathbf{x}_*)$ having operator norm less than one. Let $\mathbf{W} := \nabla\mathbf{q}(\mathbf{x}_*)$, then $\mathbf{q}(\mathbf{x})$ is locally approximated at \mathbf{x}_* by its first-order Taylor expansion $\mathbf{q}(\mathbf{x}_*) + \mathbf{W}(\mathbf{x} - \mathbf{x}_*)$. As a result of this local approximation, the fixed-point iteration has a local r -linear convergence factor of $\|\mathbf{W}\|$, and using our prior analysis we prove a modified version of AA(m) bests the local convergence of the fixed-point iteration.

The modified version of AA(m) we consider for this setting adds an additional bounding constraint on the coefficients $\alpha_j^{(k)}$. Thus, at each iteration, rather than solving (2), the following model is solved

$$\min_{\sum_{j=k-m_k}^k \alpha_j^{(k)} = 1, |\alpha_j^{(k)}| \leq C_0} \left\| \sum_{j=k-m_k}^k \alpha_j^{(k)} (\mathbf{q}(\mathbf{x}^{(j)}) - \mathbf{x}^{(j)}) \right\|, \quad (7)$$

where $C_0 > 0$ is a fixed constant. We refer to AA(m) with (2) replaced by (7) as modified AA(m). With this slight alteration, we prove the local convergence of modified AA(m) is superior to that of the fixed-point iteration.

Theorem 4 (Local convergence rate of modified AA(m) for nonlinear operators). *Assume \mathbf{x}_* is a fixed point of \mathbf{q} with $\mathbf{W} := \nabla \mathbf{q}(\mathbf{x}_*)$ symmetric, $\|\mathbf{W}\| < 1$, and $\lambda_{\max}(\mathbf{W}) \neq -\lambda_{\min}(\mathbf{W})$. Then there exists a constant C'_0 such that when $C_0 > C'_0$ and $\mathbf{x}^{(1)}$ is sufficiently close to \mathbf{x}_* , modified AA(m) converges with local r -linear convergence factor no larger than $\sqrt{w_0 \|\mathbf{W}\|}$ with $w_0 < \|\mathbf{W}\|$.*

Since the local r -linear convergence factor of the fixed-point iteration is $\|\mathbf{W}\|$, Theorem 4 implies modified AA(m) outperforms the fixed-point iteration. The proof of Theorem 4 is based on a similar argument to the proof of Theorem 1 and leverages the local first-order approximation of \mathbf{q} .

3.3.1 A Nonlinear Example: Tyler’s M-estimator

Tyler’s M-estimator (TME) (Tyler, 1987a) is a popular method for robust covariance estimation, i.e., for estimation of the covariance matrix in a way that is resistant to the influence of outliers or deviations from the assumed statistical model. This estimator is obtainable through fixed-point iterations, and we show one such formulation satisfies the symmetry assumption in Theorem 4. TME provides an important instance of a nonlinear operator to test AA(m), and we compare the performance of AA(m) to the fixed-point iterations in Section 4.

Given a data set $\{\mathbf{x}_i\}_{i=1}^n \subset \mathbb{R}^p$, the standard fixed-point iteration to compute TME is

$$\Sigma^{(k+1)} = G(\Sigma^{(k)}) := \frac{p}{n} \sum_{i=1}^n \frac{\mathbf{x}_i \mathbf{x}_i^T}{\mathbf{x}_i^T \Sigma^{(k)-1} \mathbf{x}_i}, \quad (8)$$

subject to the constraint $\text{tr}(\Sigma^{(k+1)}) = p$. Kent and Tyler (1988) established the uniqueness and existence of the underlying fixed point of (8) and its constraint, which defines the TME, along with proving convergence. Their theory holds under a natural geometric condition that avoids concentration on lower-dimensional subspaces, namely, any linear subspace of \mathbb{R}^p of dimension $1 \leq d \leq p - 1$ contains less than nd/p of the data points. Franks and Moitra (2020) established the linear convergence of (8). TME can be interpreted as the maximum likelihood estimator of the shape matrix of the angular central Gaussian distribution (Tyler, 1987b) and of the generalized elliptical distribution (Frahm and Jaekel, 2010). For data i.i.d. sampled from a continuous elliptical distribution, TME emerges as the “most robust” covariance estimator as n approaches infinity (Tyler, 1987a). The practical utility of TME is evident in multiple domains of applications (Frahm and Jaekel, 2007; Chen et al., 2011; Ollila and Koivunen, 2003; Ollila and Tyler, 2012).

An alternative iterative procedure for solving for the TME was introduced by Zhang et al. (2016).

They showed an equivalent fixed-point iteration for TME is given by

$$\mathbf{w}^{(k)} = \mathbf{F}(\mathbf{w}^{(k-1)}), \quad (9)$$

where $\mathbf{F} : \mathbb{R}^n \rightarrow \mathbb{R}^n$ and the j -th component of \mathbf{F} is given by

$$F_j(\mathbf{w}) = -\log \left(\mathbf{x}_j^T \left(\frac{p}{n} \sum_{i=1}^n e^{w_i} \mathbf{x}_i \mathbf{x}_i^T \right)^{-1} \mathbf{x}_j \right). \quad (10)$$

One can quickly verify the equivalence by letting

$$\Sigma^{(k)} = \frac{p}{n} \sum_{i=1}^n e^{w_i^{(k)}} \mathbf{x}_i \mathbf{x}_i^T. \quad (11)$$

Then (10) implies

$$w_j^{(k+1)} = -\log(\mathbf{x}_j^T \Sigma^{(k)-1} \mathbf{x}_j), \quad (12)$$

and from these equations one can obtain the standard fixed-point iteration. Notably, however, though these iterations are equivalent, the standard iterative procedure fails to have a symmetric Jacobian at fixed points while the alternative procedure does. The next lemma proves this fact. Since our numerical results directly apply this lemma and its proof is short, we include it here.

Lemma 5. *Let \mathbf{w}^* be a fixed point of (9). Then, $\nabla \mathbf{F}(\mathbf{w}^*)$ is symmetric.*

Proof. At the fixed point \mathbf{w}^* we have $w_j^* = -\log \left(\mathbf{x}_j^T \left(\frac{p}{n} \sum_{i=1}^n e^{w_i^*} \mathbf{x}_i \mathbf{x}_i^T \right)^{-1} \mathbf{x}_j \right)$ which implies

$$\mathbf{x}_j^T \left(\frac{p}{n} \sum_{i=1}^n e^{w_i^*} \mathbf{x}_i \mathbf{x}_i^T \right)^{-1} \mathbf{x}_j = e^{-w_j^*}. \quad (13)$$

From (11), (12), and (13) it follows $e^{w_j^*} = \frac{1}{\mathbf{x}_j^T \Sigma^{*-1} \mathbf{x}_j}$. Therefore,

$$\frac{d}{dw_i} F_j(\mathbf{w}^*) = \frac{\mathbf{x}_j^T \Sigma^{*-1} \left(\frac{p}{n} e^{w_i^*} \mathbf{x}_i \mathbf{x}_i^T \right) \Sigma^{*-1} \mathbf{x}_j}{\mathbf{x}_j^T \Sigma^{*-1} \mathbf{x}_j} = e^{w_j^*} \mathbf{x}_j^T \Sigma^{*-1} \left(\frac{p}{n} e^{w_i^*} \mathbf{x}_i \mathbf{x}_i^T \right) \Sigma^{*-1} \mathbf{x}_j$$

from which we see $\frac{d}{dw_i} F_j(\mathbf{w}^*) = \frac{d}{dw_j} F_i(\mathbf{w}^*)$ for all i and j . □

3.4 Discussion of Results

Our work establishes an upper bound on the r -linear convergence factor of AA(m) which we show in many cases to be strictly less than the convergence factor of the fixed-point iteration. This result is a new addition to the literature because we directly show AA(m) has a better rate which prior works have not clearly demonstrated (Evans et al., 2020; De Sterck and He, 2022; Pollock and Rebholz, 2021; Pollock et al., 2019).

Our analysis studied the improvement of AA(m) over every pair of iterations, and we see the estimates we derived can be tight. In Section 4, we show in our numerical experiments our estimation in (4) is usually tight for AA(1). In practice, we observe the improvement factor varies over iterations, see Figures 2 and 4, which results in a smaller r-linear convergence factor asymptotically. Additionally, we have noted the improvement factor appears to depend upon m ; therefore, we conjecture our estimation of the r-linear convergence factor could be improved by investigating the improvement of AA over more consecutive iterations. We also expect faster convergence rates when $m \geq 2$, improving from our current estimation that is independent of m . For example, Proposition 3 already shows that there are some settings where AA(m) with $m \geq 2$ has an improved convergence factor over $m = 1$, and existing results (Scieur, 2019) establish the convergence factor when m is infinite, which is numerically smaller than our rate of $\sqrt{w_0} \|\mathbf{W}\|$. We refer the reader to the acceleration monograph by d’Aspremont et al. (2021) for a complete review. We remark that while it is possible to apply these results to analyze the convergence of Anderson acceleration with restarts after every m steps (Bertrand and Massias, 2021, Eqn (3)), their analysis does not apply to the setting of work, which analyzes AA with a moving window of points of depth m .

As a closing remark, in practice it is common to apply a damping technique in AA(m), that is, instead of (3), the next iterate is updated as

$$\mathbf{x}^{(k+1)} = \beta \sum_{j=k-m_k}^k \alpha_j^{(k)} \mathbf{q}(\mathbf{x}^{(j)}) + (1 - \beta) \sum_{j=k-m_k}^k \alpha_j^{(k)} \mathbf{x}^{(j)}$$

for some $\beta \in [0, 1]$. If this technique is applied, similar results to ours can be obtained. For example, Theorem 1 and Proposition 3 hold by replacing \mathbf{W} with $\beta\mathbf{W} + (1 - \beta)\mathbf{I}$.

4 Simulations

We investigated our theoretical results with numerical experiments on symmetric linear and nonlinear operators in Sections 4.1 and 4.2 respectively. We also compared and discussed three different variants of AA in Section 4.3 for TME. Our numerical experiments provide empirical support for our theoretical results and demonstrate the exciting effectiveness of AA(m) for TME.

4.1 Linear Symmetric Operators

We conducted numerical experiments on linear operators $\mathbf{q}(\mathbf{x}) = \mathbf{W}\mathbf{x} + \mathbf{a}$, where \mathbf{W} is symmetric and $\|\mathbf{W}\| < 1$, and verified the tightness of the upper bound on the r -linear convergence factor proven in Theorem 1. We present two experiments; the first verifies the tightness of (4); the second displays the upper bound on the r-linear convergence factor for AA(m).

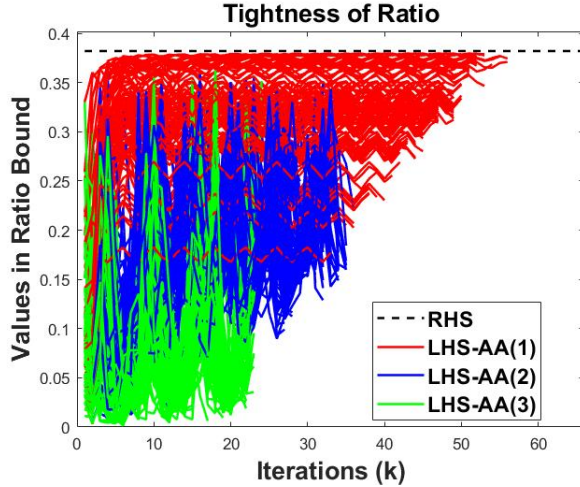


Figure 2: Presents the left-hand side of (4) for all iterations $k \geq 2$ for one hundred random initializations of AA(m), for $m = 1, 2, 3$, with $\mathbf{q}_1(\mathbf{x}) = \mathbf{W}_1\mathbf{x}$ and $\mathbf{W}_1 = \text{Diag}([-0.07, 0.62, -0.55, -0.6, 0.15])$; LHS-AA(m) denotes the value of the left-hand side of (4) for the iterates of AA(m) for each random initialization while the dotted black line shows the constant right-hand side (RHS) of (4).

For experiment one, we let $\mathbf{W}_1 = \text{Diag}([-0.07, 0.62, -0.55, -0.6, 0.15])$ and defined $\mathbf{q}_1(\mathbf{x}) := \mathbf{W}_1\mathbf{x}$. We computed the fixed point of \mathbf{q}_1 with AA(m) for $m = 1, 2$, and 3 and checked inequality (4) for the iterates generated by AA(m) for one hundred random initializations of each algorithm. Each instance of AA(m) terminated once the fixed-point error, i.e., $\|\mathbf{q}_1(\mathbf{x}) - \mathbf{x}\|$, was less than 10^{-12} . The random initial vectors for AA(m) had entries drawn from a standard normal. Figure 2 displays the results of this experiment.

We observe in Figure 2 that the value of the left-hand side of (4) was always bounded by the right-hand side. The set of iterates generated by AA(1) obtained the minimum gap of 0.0024 between the left and right-hand sides of (4). In relative terms, the minimum gap was 0.62% of the value of the right-hand side which strongly supports the tightness of the inequality.

Our second experiment demonstrates the upper bound on the r-linear convergence factor for AA(m) provided by Theorem 1. For this experiment, we randomly generated $\mathbf{W}_2 \in \mathcal{S}^{500 \times 500}$ with all but the smallest eigenvalue drawn uniformly at random between -0.9 and 0.9; the smallest eigenvalue was chosen to be -0.95. We applied the fixed-point iteration (FP) and AA(m) to solve $\mathbf{q}_2(\mathbf{x}) := \mathbf{W}_2\mathbf{x}$ from one hundred random initializations. We used the same initialization process and termination criteria as in the first experiment. The r-linear convergence factor was estimated as

$$r_{est}(k) := \max_{n \geq k} \|\mathbf{x}_* - \mathbf{x}^{(n)}\|^{1/n}. \quad (14)$$

Figure 3 displays the results of the numerical experiment. The figure shows that the predicted

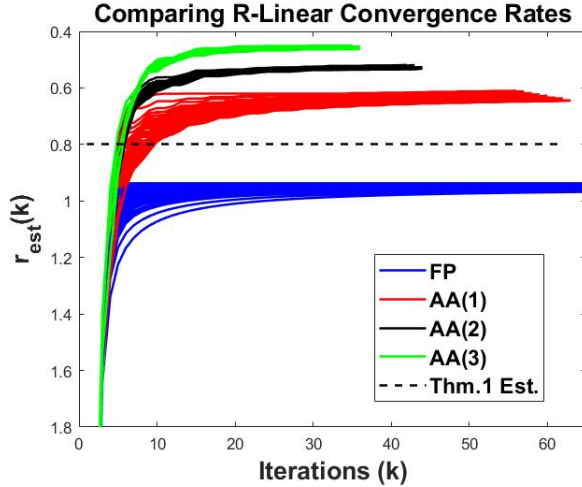


Figure 3: Displays the estimated r-linear convergence factors for FP and AA(m) for the linear operator $\mathbf{q}_2(\mathbf{x}) = \mathbf{W}_2\mathbf{x}$ for one hundred random initializations of each method. The dashed line is the upper-bound on the r-linear convergence factor from Theorem 1.

bound on the r-linear convergence factor is both an upper bound on the performance of AA(m) and is a strict lower bound on the performance of the fixed-point iteration. Additionally, it shows the r-linear convergence factors for AA(m) depend on the initialization, as observed in the literature, and that the convergence factor improves as m increases.

4.2 Nonlinear operator

For our nonlinear operator experiments we investigated AA(m) applied to TME as described in Section 3.3.1. For our experiments we utilized two data models:

Data Model 1: Letting $(S_p)_{ij} = (0.7)^{|i-j|}$, data points were generated as $\mathbf{x}_i = \mathbf{S}_p^{1/2}\boldsymbol{\zeta}$ where $\zeta_i \sim \mathcal{N}(0, 1)$; we generated 110 data points with $\mathbf{x}_i \in \mathbb{R}^{100}$; see Section 7.1 of Goes et al. (2020) for a full description of this model.

Data Model 2: This model is an inlier-outlier model containing 997 data points in \mathbb{R}^{100} . The data matrix \mathbf{X} , whose columns form the data set $\{\mathbf{x}_i\}_{i=1}^n$, was formed as

$$\mathbf{X} = \begin{pmatrix} \text{randn}(n_0, D) \cdot \text{randn}(D, D) \\ [\text{randn}(n_1, d)/\sqrt{d} \mid \mathbf{0}] \end{pmatrix}^\top,$$

where $n_0 = 500$, $n_1 = 497$, $D = 100$, $d = 50$, and $\text{randn}(m, n)$ forms an m -by- n matrix with entries drawn from a standard normal.

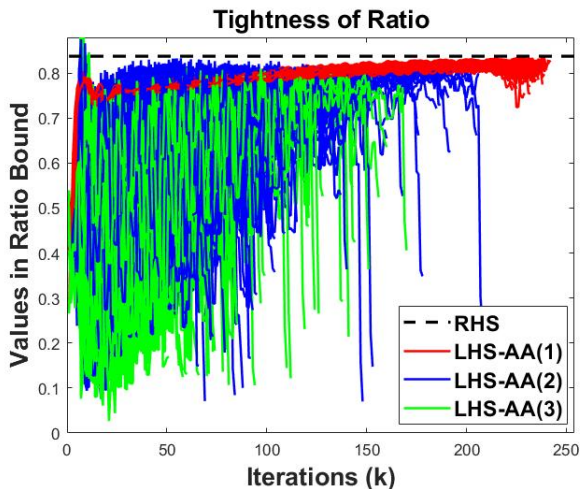


Figure 4: Displays the value of the LHS of (41) for iterates generated by AA(m) for one hundred random initializations for an instance of Data Model 1. LHS-AA(m) denotes the value of the LHS of (41) for the iterates of AA(m); the black dotted line is the RHS of (41).

We begin with numerical tests on Data Model 1. Our first experiment compared the alternative TME fixed-point iteration to AA(m) applied to (10) for an instance of Data Model 1 to verify the theoretical results while the second and third experiments display the superior performance of AA(m) over the standard TME fixed-point method.

In the first experiment, each method was randomly initialized one hundred times, and all methods were terminated once the fixed-point error was less than 10^{-12} . To fairly estimate the r-linear convergence factor of the methods, we first computed the unique solution to the TME having trace equal to $p = 100$. The estimates of the r-linear convergence factors for each method were then computed from (14) by using (11) to transform each vector iterate, $\mathbf{w}^{(k)}$, into a matrix which was then scaled to have trace equal to p .

The reason for this estimation of the r-linear convergence factor follows from the scale-invariance of the TME, i.e., \mathbf{F} has multiple fixed points: if \mathbf{w}_* is a fixed point then $\mathbf{w}_* + \mathbf{c}$, with constant vector \mathbf{c} , is a fixed point. The scale-invariance also causes $\mathbf{W} := \nabla \mathbf{F}(\mathbf{w}_*)$, with \mathbf{w}_* a fixed point of (10), to have an eigenvalue of 1 with a constant eigenvector. As a result, we use the second largest eigenvalue of \mathbf{W} to calculate the right-hand side of (41) and the upper bound on the r-linear convergence factor for AA(m). We observe this generates accurate bounds in our experiments.

Figures 4 and 5 present the results of the numerical experiment performed on Data Model 1. We observe in Figure 4 the right-hand side of (41) serves as an upper bound on the improvement ratio. Our theory predicts the bound will hold for all iterates sufficiently close to a solution and the

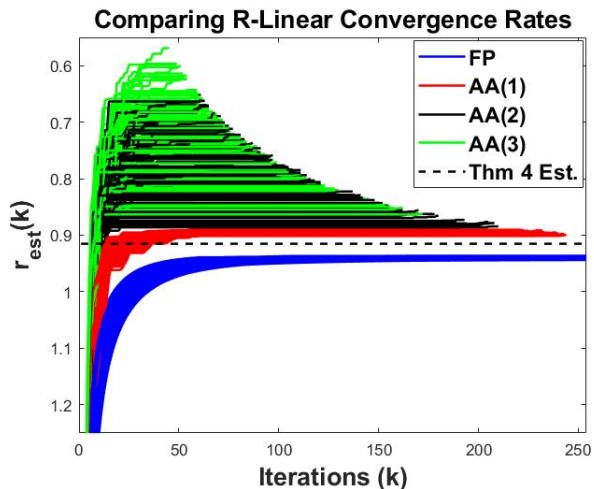


Figure 5: Displays the estimated r-linear convergence rates of AA(m) applied to (10) and the alternative TME fixed-point iteration for one hundred random initializations of the methods for an instance of Data Model 1. The dashed line is the upper-bound on the r-linear convergence factor given by Theorem 4.

figure supports this. Figure 5 clearly presents that the upper bound on the r-linear convergence factor given by Theorem 4 holds; AA(m) for $m = 1, 2$, and 3 all out-perform the estimate while the fixed-point scheme given by (10) has an r-linear factor larger than the given estimate.

We next present two numerical tests which compare the computational expense and performance of AA(m) and the standard TME fixed-point iteration on Data Model 1. We utilized the standard TME fixed-point iteration over the alternative approach when comparing computational time and cost because we found the fixed-point iteration given by (8) outperformed (10) on these measures. As before, we solved ten different instantiations of Data Model 1 from ten different random initializations of our methods. The two settings of Data Model 1 we considered were $(p, n) = (100, 110)$ and $(p, n) = (200, 210)$. Each method ran until the fixed-point error was less than or equal to 10^{-12} . Figures 6 and 7 display the results of the numerical experiments. From the figures, we see that in all of the tests AA(m) required less iterations to compute a solution to the desired tolerance. For the setting $(p, n) = (100, 110)$, AA(3) always obtained a solution faster than the fixed-point iteration while AA(2) computed a solution slower one time in all of the one hundred experiments. The results were similar for $(p, n) = (200, 210)$. In this setting, AA(2) and AA(3) computed solutions faster than the fixed-point approach in all tests, and the fixed-point iteration only computed a solution faster than AA(1) in two tests. Thus, these experiments demonstrate AA provides a powerful method for solving the TME and can significantly outperform the standard fixed-point schemes.

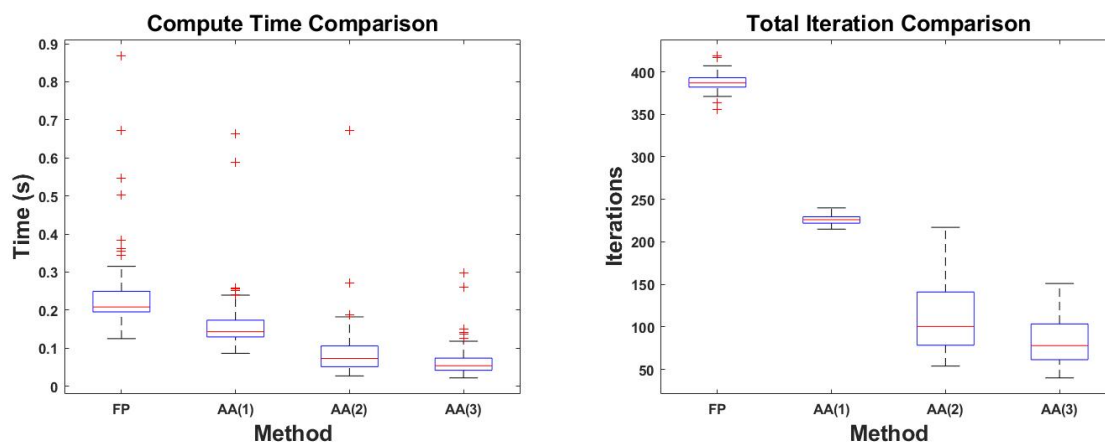


Figure 6: Displays boxplots for the computational time and total iterations required to solve TME with the standard TME fixed-point iteration (FP) and AA(m) applied to the alternative TME fixed-point iteration for Data Model 1 with $(p, n) = (100, 110)$.

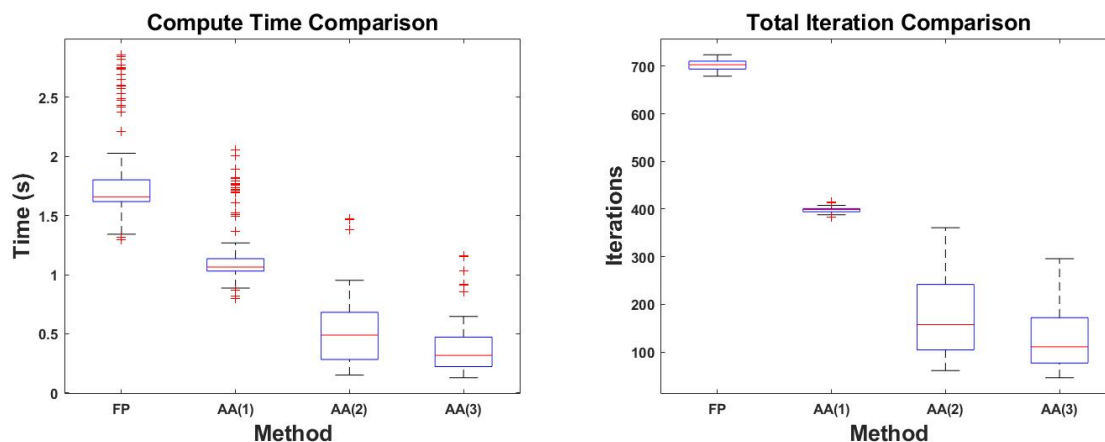


Figure 7: Displays boxplots for the computational time and total iterations required to solve TME with the standard TME fixed-point iteration (FP) and AA(m) applied to the alternative TME fixed-point iteration for Data Model 1 with $(p, n) = (200, 210)$.

Data Model 2 was used in our second set of experiments. We solved ten different instantiations of the model with ten different random initializations of each approach for a total of one hundred implementations of each method. All algorithms were terminated when the fixed-point error was less than 10^{-12} .

The results of the numerical tests are presented in Figure 8 with a set of box-plots. The figure clearly demonstrates AA(1), AA(2), and AA(3) computed solutions to TME faster than the standard fixed-point iteration for all experiments with AA(m) converging nearly ten-times faster in every

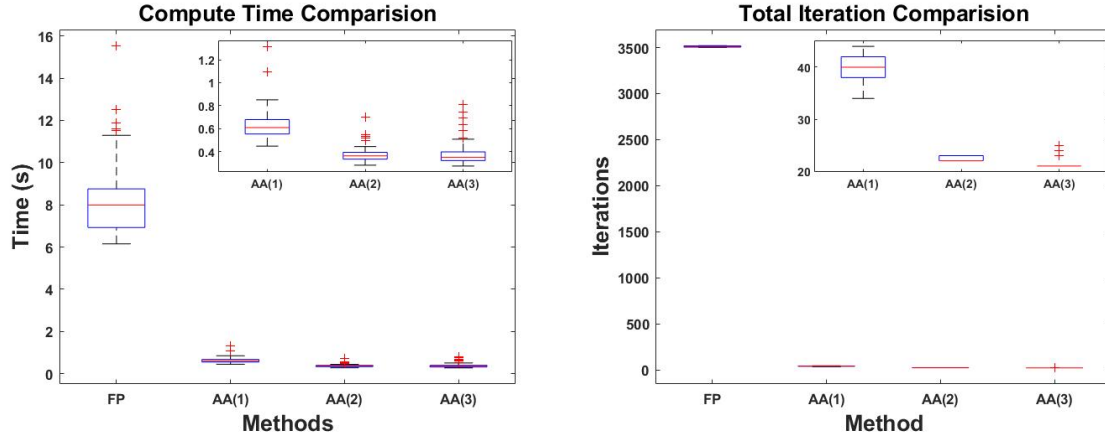


Figure 8: Presents a box-plot of the iterations and time required for each method to compute a solution for Tyler’s M-estimation with Data Model 2; FP refers to the fixed-point iteration (8) with scaled iterate to have trace equal to p while AA(m) references AA(m) applied to (10).

test. The comparison for Data Model 2 was even more striking than for Data Model 1. In this inlier-outlier setting, the fixed-point method was completely outclassed by AA(m); therefore, this suggests AA(m) can prove to be a great benefit in settings where the standard fixed-point approach exhibits slow linear convergence.

Besides investigating the computational advantage of AA(m), we further validated the strength of our theory in the non-linear setting. Figure 9 compares the r-linear convergence factor of AA(m) to the standard TME fixed-point iteration and displays the bound in (41) for the experiments displayed in Figure 8. Figure 8 clearly demonstrated AA vastly decreased the compute time, and the right panel in Figure 9 gives some evidence as to why. The r-linear convergence factors of AA(2) and AA(3) in the one hundred experiments were approximately 0.4 while the r-linear convergence factor of the standard TME fixed-point iteration was about one. As discussed in Section 3.4, we note the closeness of the estimate of the r-linear convergence factor to the fixed-point method’s rate suggests our theory can further be refined to achieve a better bound. This might be achieved by investigating the improvement of AA(m) over more iterations than currently investigated in our analysis.

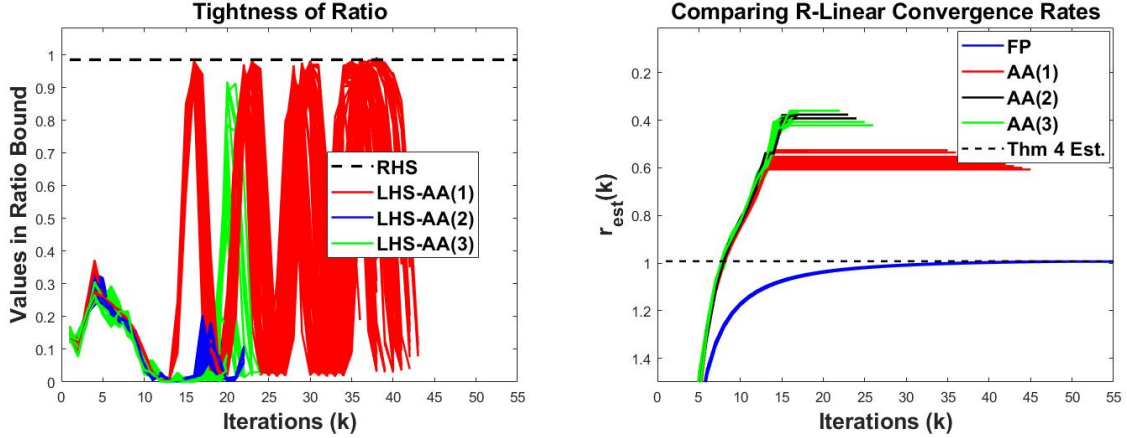


Figure 9: Displays the results of the hundred random experiments conducted on Data Model 2. The panel on the left displays the value of the LHS of (41) for iterates generated by $AA(m)$ applied to (10). The panel on the right displays the estimated r -linear convergence rates of $AA(m)$ applied to the alternative TME fixed-point iteration. The dashed line is the upper-bound on the r -linear convergence factor given by Theorem 4.

4.3 Comparison of Anderson Acceleration Variants for TME

As mentioned earlier, many different variants of AA exist and are studied in the literature. The three most popular AA variants are the following ones.

Full-memory AA utilizes all prior iterates to compute the next iterate. Setting $m = \infty$ in Algorithm 1 is equivalent to this approach, so we denote it as $AA(\infty)$.

Restarting AA operates as full-memory AA until a certain number of fixed iterations m is reached at which point in time the method clears its memory and begins anew with the last iterate as a new initialization; we denote this version as $\text{restart-AA}(m)$.

Windowed AA, with window size m , is $AA(m)$ as defined in Algorithm 1.

For discussions on these methods and their analysis see the aforementioned references. Now, the different variants of AA do not always behave in manners which are easy to understand. To illustrate this, we applied all three AA variants to the two TME Data models from Section 4.2. The results can be viewed in Figure 10. For Data Model 1, restarting AA with $m = 2$ performed just as good as full-memory AA and was significantly better than windowed AA with $m = 2$; however, the roles were reversed when the methods were applied to the inlier-outlier data model, Data Model 2. In this setting, windowed AA was clearly better while restarting AA appeared to alternate between different rates of convergence. We do not presently have a clear explanation

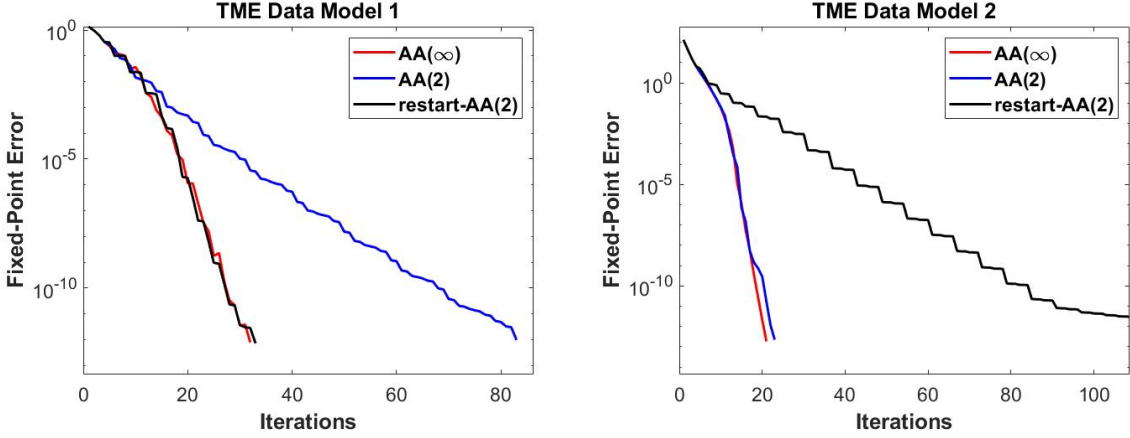


Figure 10: Displays the results of comparing full-memory AA, restarting AA, and windowed AA on the TME problem with Data Models 1 and 2. The fixed-point error is the norm of the difference of the consecutive iterates of each method.

for the difference in the behavior between the two methods though we suspect the phenomenon is highly problem dependent. This could be a fruitful direction to explore in the future.

5 Technical Proofs

5.1 Proof of Theorem 1

Proof. As described in Section 3.2, we may assume without loss of generality $\mathbf{a} = \mathbf{0}$, $\mathbf{x}_* = \mathbf{0}$, and reformulate AA(m) as the following iterative process:

1. Let $\tilde{\mathbf{y}}^{(k+1)}$ be the point on the affine subspace spanned by $\tilde{\mathbf{x}}^{(k-m_k)}, \dots, \tilde{\mathbf{x}}^{(k)}$ with the smallest norm, $\|\tilde{\mathbf{y}}^{(k+1)}\|^2$
2. $\tilde{\mathbf{x}}^{(k+1)} = \mathbf{q}(\tilde{\mathbf{y}}^{(k+1)})$

where $m_k := \min(m, k)$ and we assumed in our derivation of the reformulation $\tilde{\mathbf{x}}^{(k)} = \mathbf{q}(\mathbf{x}^{(k)}) - \mathbf{x}^{(k)}$. We first verify (4). We begin by noting (4) is equivalent to

$$\frac{\|\tilde{\mathbf{x}}^{(k+1)}\|}{\|\tilde{\mathbf{x}}^{(k-1)}\|} \leq w_0 \|\mathbf{W}\|.$$

Since $\tilde{\mathbf{x}}^{(k+1)} = \mathbf{q}(\tilde{\mathbf{y}}^{(k+1)})$ by Step 2 it follows $\|\tilde{\mathbf{x}}^{(k+1)}\| \cdot \|\mathbf{W}\|^{-1} \leq \|\tilde{\mathbf{y}}^{(k+1)}\|$. Therefore, to prove (4) it is sufficient to show

$$\frac{\|\tilde{\mathbf{y}}^{(k+1)}\|}{\|\tilde{\mathbf{x}}^{(k-1)}\|} \leq w_0. \quad (15)$$

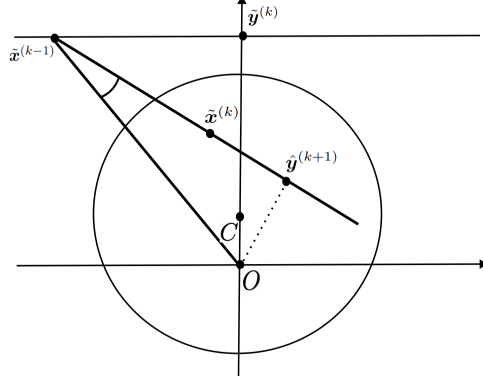


Figure 11: A visualization of $\tilde{\mathbf{x}}^{(k-1)}$, $\tilde{\mathbf{x}}^{(k)}$, $\tilde{\mathbf{y}}^{(k)}$, and $\hat{\mathbf{y}}^{(k+1)}$. The ball with center C represents the region defined by Lemma 6 showing the possible values of $\mathbf{W}\tilde{\mathbf{y}}^{(k)}$.

We now demonstrate this relationship holds. Let $\hat{\mathbf{y}}^{(k+1)}$ be the projection of the origin to the line connecting $\tilde{\mathbf{x}}^{(k-1)}$ and $\tilde{\mathbf{x}}^{(k)}$, thereby making it a linear combination of $\tilde{\mathbf{x}}^{(k-1)}$ and $\tilde{\mathbf{x}}^{(k)}$. Then by the definition of $\tilde{\mathbf{y}}^{(k+1)}$ in Step 1 we have

$$\|\hat{\mathbf{y}}^{(k+1)}\| \geq \|\tilde{\mathbf{y}}^{(k+1)}\| \quad (16)$$

and

$$\frac{\|\hat{\mathbf{y}}^{(k+1)}\|}{\|\tilde{\mathbf{x}}^{(k-1)}\|} = \sin \angle(\mathbf{O}\tilde{\mathbf{x}}^{(k-1)}\hat{\mathbf{y}}^{(k+1)}) = \sin \angle(\mathbf{O}\tilde{\mathbf{x}}^{(k-1)}\tilde{\mathbf{x}}^{(k)}). \quad (17)$$

By (16) and (17) it follows, if we prove $\sin \angle(\mathbf{O}\tilde{\mathbf{x}}^{(k-1)}\tilde{\mathbf{x}}^{(k)}) \leq w_0$, then we will have proven our claim. To help bound the sine of this angle, we introduce the following lemma:

Lemma 6. *For any symmetric matrix \mathbf{W} , $\mathbf{W}\mathbf{x}$ lies in the ball centered at $(\lambda_{\max}(\mathbf{W}) + \lambda_{\min}(\mathbf{W}))\mathbf{x}/2$ with radius $(\lambda_{\max}(\mathbf{W}) - \lambda_{\min}(\mathbf{W}))\|\mathbf{x}\|/2$.*

Proof. Given any $\mathbf{W} \in \mathcal{S}^{n \times n}$ and $\mathbf{x} \in \mathbb{R}^n$, we see

$$\begin{aligned} \|\mathbf{W}\mathbf{x} - \frac{1}{2}(\lambda_{\max}(\mathbf{W}) + \lambda_{\min}(\mathbf{W}))\mathbf{x}\| &\leq \|\mathbf{W} - \frac{1}{2}(\lambda_{\max}(\mathbf{W}) + \lambda_{\min}(\mathbf{W}))\mathbf{I}\| \cdot \|\mathbf{x}\| \\ &= \frac{1}{2}(\lambda_{\max}(\mathbf{W}) - \lambda_{\min}(\mathbf{W}))\|\mathbf{x}\|. \end{aligned}$$

□

We now utilize a geometric argument. First, we note without loss of generality we may assume $\tilde{\mathbf{y}}^{(k)} = [0, 1, 0, \dots, 0]$. Then following the definition of $\tilde{\mathbf{y}}^{(k)}$, $\tilde{\mathbf{x}}^{(k-1)} - \tilde{\mathbf{y}}^{(k)}$ is perpendicular to $\tilde{\mathbf{y}}^{(k)}$, and $\tilde{\mathbf{x}}^{(k-1)}$ must lie on the hyperplane through the point $(0, 1, 0, \dots, 0)$ with normal vector being the second standard basis vector in \mathbb{R}^n . Note, we may assume this by applying a unitary

transformation and scaling all points $\tilde{\mathbf{x}}^{(j)}$, $j = k - m_k, \dots, k$, which form $\tilde{\mathbf{y}}^{(k)}$. Furthermore, by unitary transformation we may also assume $\tilde{\mathbf{x}}^{(k-1)} - \tilde{\mathbf{y}}^{(k)}$ is parallel to the first standard basis vector in \mathbb{R}^n . A geometric representation of our transformed problem, presenting the relationship between $\tilde{\mathbf{x}}^{(k-1)}$, $\tilde{\mathbf{x}}^{(k)}$, $\tilde{\mathbf{y}}^{(k)}$, and $\hat{\mathbf{y}}^{(k+1)}$, is given in Figure 11. Using Lemma 6, we denote in Figure 11 all the possible values of $\tilde{\mathbf{x}}^{(k)} = \mathbf{W}\tilde{\mathbf{y}}^{(k)}$, which is given by all the points contained in the ball centered at $C = (\lambda_{\max}(\mathbf{W}) + \lambda_{\min}(\mathbf{W}))\tilde{\mathbf{y}}^{(k)}/2$ with radius

$$r := (\lambda_{\max}(\mathbf{W}) - \lambda_{\min}(\mathbf{W}))\|\tilde{\mathbf{y}}^{(k)}\|/2 = (\lambda_{\max}(\mathbf{W}) - \lambda_{\min}(\mathbf{W}))/2.$$

Our aim is to bound $\angle(\mathbf{O}\tilde{\mathbf{x}}^{(k-1)}\tilde{\mathbf{x}}^{(k)})$, which we realize is maximized when $\tilde{\mathbf{x}}^{(k)}$ is on the sphere centered at C with radius r such that the line connecting $\tilde{\mathbf{x}}^{(k-1)}$ and $\tilde{\mathbf{x}}^{(k)}$ is tangent to the sphere. As a result, the value of $\tilde{\mathbf{x}}^{(k)}$ which maximizes $\angle(\mathbf{O}\tilde{\mathbf{x}}^{(k-1)}\tilde{\mathbf{x}}^{(k)})$ lies in a 2-dimensional plane containing $\tilde{\mathbf{x}}^{(k)}$ and $\tilde{\mathbf{y}}^{(k)}$. A visualization of this setting is depicted in Figure 12. Note, another possible orientation of the figure has C below the x -axis. Then the visualization would be different as the line connecting $\tilde{\mathbf{x}}^{(k-1)}$ and $\tilde{\mathbf{x}}^{(k)}$ will be the other tangent line; however, the argumentation for this setting is analogous and does not alter the derivation of w_0 .

The setting represented by Figure 12 is identical to Figure 1 in Section 3.1, with $P = \tilde{\mathbf{x}}^{(k-1)}$, $R = \tilde{\mathbf{y}}^{(k)}$, $Q = \tilde{\mathbf{x}}^{(k)}$. As a result, the argument presented in Section 3.1 following the statement of Theorem 1 holds and w_0 is as defined in (3). Therefore, following our previous discussion, $\sin \angle(\mathbf{O}\tilde{\mathbf{x}}^{(k-1)}\tilde{\mathbf{x}}^{(k)}) \leq w_0$ for all possible $\tilde{\mathbf{x}}^{(k)}$, i.e., all points inside in the ball specified by Lemma 6, which proves (4).

Since $\|\mathbf{W}\| < 1$, we know the sequence $\{\tilde{\mathbf{x}}^{(k)}\}$ converges to $\mathbf{x}_* = \mathbf{0}$. Using (4), we see the r-linear convergence factor is bounded by $\sqrt{w_0\|\mathbf{W}\|}$. From (4) it follows

$$\|\tilde{\mathbf{x}}^{(k)}\| \leq w_0\|\mathbf{W}\|\|\tilde{\mathbf{x}}^{(k-2)}\| \leq (w_0\|\mathbf{W}\|)^2\|\tilde{\mathbf{x}}^{(k-4)}\| \leq \dots \leq (w_0\|\mathbf{W}\|)^{\lfloor (k-2)/2 \rfloor + 1} \max\left(\|\tilde{\mathbf{x}}^{(0)}\|, \|\tilde{\mathbf{x}}^{(1)}\|\right),$$

and so

$$\rho_{\{\tilde{\mathbf{x}}^{(k)}\}} = \limsup_{k \rightarrow \infty} \|\tilde{\mathbf{x}}^{(k)}\|^{1/k} \leq \lim_{k \rightarrow \infty} \left((w_0\|\mathbf{W}\|)^{\lfloor (k-2)/2 \rfloor + 1} \max\left(\|\tilde{\mathbf{x}}^{(0)}\|, \|\tilde{\mathbf{x}}^{(1)}\|\right) \right)^{1/k} = \sqrt{w_0\|\mathbf{W}\|}.$$

Lastly, we prove $w_0 \leq \|\mathbf{W}\|$, with equality holding if and only if $\lambda_{\max}(\mathbf{W}) = -\lambda_{\min}(\mathbf{W})$. Using our geometric understanding of the problem in Figure 1, we note

$$\sin \angle(OPQ) = \frac{\text{dist}(O, L)}{|OP|},$$

where L represents the line connecting P and Q . Looking at the terms in this ratio we see

$$|OP| \geq |OR| = 1 \tag{18}$$

and

$$\text{dist}(O, L) \leq |OC| + \text{dist}(C, L) = |OC| + |CQ| = \|\mathbf{W}\| \tag{19}$$

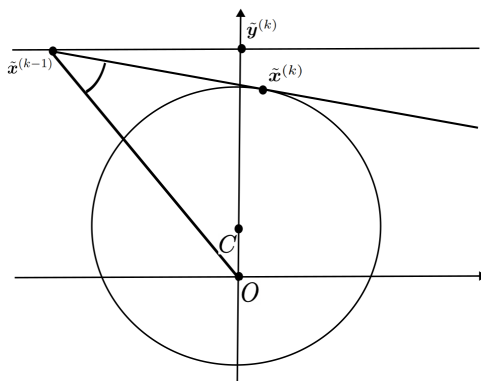


Figure 12: A visualization when $\angle(O\tilde{\mathbf{x}}^{(k-1)}\tilde{\mathbf{x}}^{(k)})$ is at its maximum.

and so it follows that $\sin \angle(OPQ) \leq \|\mathbf{W}\|$; therefore, since w_0 is the largest possible $\sin \angle(OPQ)$, we have $w_0 \leq \|\mathbf{W}\|$. From the argument above, $w_0 = \|\mathbf{W}\|$ only when (18) and (19) are equalities, that is, $P = R$ and O, C, Q are collinear. If $C \neq O$, then the collinearity of O, C, Q implies that Q must lie on the y -axis in Figure 1; however, this would violate the required tangency of L with the circle. As a result, $w_0 = \|\mathbf{W}\|$ will only occur in this problem provided $O = C$, i.e., $\lambda_{\min}(\mathbf{W}) + \lambda_{\max}(\mathbf{W}) = 0$. On the other hand, when $\lambda_{\min}(\mathbf{W}) + \lambda_{\max}(\mathbf{W}) = 0$, we have $C = O$ in Figure 1 and the circle has a radius of $\|\mathbf{W}\|$. Let $a \rightarrow \infty$ in (3), i.e., $P = R$ in Figure 1, it follows that $\sin \angle(OPQ) = \|\mathbf{W}\|$; therefore, $w_0 = \|\mathbf{W}\|$. \square

5.2 Proof of Proposition 2

Proof. Let $\mathbf{W} = w\mathbf{I}$ with $|w| < 1$. We define $\tilde{\mathbf{y}}^{(k)}$ and $\tilde{\mathbf{x}}^{(k)}$ as discussed in the proof of Theorem 1 and assume without loss of generality $\tilde{\mathbf{y}}^{(k)} = [0, 1, 0, \dots, 0]$ and that $\tilde{\mathbf{x}}^{(k-1)}$ lies on the hyperplane through the point $(0, 1, 0, \dots, 0)$ with normal vector parallel to the second standard basis vector in \mathbb{R}^n . Given the geometric meaning of w_0 discussed in Section 3.1 and in the proof of Theorem 1, it suggests the circle in Figure 11 has radius 0 and is reduced to a point centered at $C = w\tilde{\mathbf{y}}^{(k)}$, and w_0 is equivalent to finding a point P on the line $y = 1$ such that $\angle(OPC)$ is the largest and O is the origin. Let $R = (0, 1)$ and $|PR| = 1/a$ with $a > 0$. Then,

$$\angle(OPC) = \angle(OPR) - \angle(CPR) = \tan^{-1}(a) - \tan^{-1}((1 - \|\mathbf{W}\|)a),$$

and taking the derivative with respect to a we see the maximum angle is achieved when

$$\frac{1}{1+a^2} = \frac{(1 - \|\mathbf{W}\|)}{1 + (1 - \|\mathbf{W}\|)^2 a^2}, \text{ that is, } a = \frac{1}{\sqrt{1 - \|\mathbf{W}\|}}.$$

Then,

$$\begin{aligned}\sin(\angle(OPC)) &= \sin\left(\tan^{-1}\frac{1}{\sqrt{1-\|\mathbf{W}\|}}\right)\cos(\tan^{-1}\sqrt{1-\|\mathbf{W}\|}) \\ &\quad - \cos\left(\tan^{-1}\frac{1}{\sqrt{1-\|\mathbf{W}\|}}\right)\sin(\tan^{-1}\sqrt{1-\|\mathbf{W}\|}) \\ &= \frac{1}{\sqrt{2-\|\mathbf{W}\|}}\frac{1}{\sqrt{2-\|\mathbf{W}\|}} - \frac{\sqrt{1-\|\mathbf{W}\|}}{\sqrt{2-\|\mathbf{W}\|}}\frac{\sqrt{1-\|\mathbf{W}\|}}{\sqrt{2-\|\mathbf{W}\|}}\end{aligned}$$

and therefore $w_0 = \|\mathbf{W}\|/(2 - \|\mathbf{W}\|)$.

Next, we show when AA(1) is applied to this problem with a specific initialization that (4) is equality. For this argument, a visualization is provided in Figure 13. Let $\theta^{(k)} = \angle(\tilde{\mathbf{y}}^{(k)}\tilde{\mathbf{x}}^{(k-1)}O)$ and $\theta^{(k+1)} = \angle(\tilde{\mathbf{y}}^{(k+1)}\tilde{\mathbf{x}}^{(k)}O)$. Then,

$$\tan\theta^{(k+1)} = \tan\angle(\tilde{\mathbf{y}}^{(k+1)}\tilde{\mathbf{x}}^{(k)}O) = \tan\angle(\tilde{\mathbf{y}}^{(k)}\tilde{\mathbf{x}}^{(k)}\tilde{\mathbf{x}}^{(k-1)}) = \frac{\|\tilde{\mathbf{y}}^{(k)} - \tilde{\mathbf{x}}^{(k-1)}\|}{(1-w)\|\tilde{\mathbf{y}}^{(k)}\|} = \frac{1}{(1-w)\tan\theta^{(k)}}, \quad (20)$$

and as a result $\theta^{(k)} = \theta^{(k+2)}$ for all $k \geq 1$. In addition, $\|\tilde{\mathbf{x}}^{(k)}\|/\|\tilde{\mathbf{x}}^{(k-1)}\| = w\|\tilde{\mathbf{y}}^{(k)}\|/\|\tilde{\mathbf{x}}^{(k-1)}\| = w \sin\theta^{(k)}$; therefore, it follows that

$$\frac{\|\tilde{\mathbf{x}}^{(k+1)}\|}{\|\tilde{\mathbf{x}}^{(k-1)}\|} = \frac{\|\tilde{\mathbf{x}}^{(k+1)}\|}{\|\tilde{\mathbf{x}}^{(k)}\|} \cdot \frac{\|\tilde{\mathbf{x}}^{(k)}\|}{\|\tilde{\mathbf{x}}^{(k-1)}\|} = w^2 \sin\theta^{(k+1)} \sin\theta^{(k)} = w^2 \sin\theta^{(1)} \sin\theta^{(2)}$$

making the left-hand side of (4) constant for all k , and equality will be obtained provided $\mathbf{x}^{(0)}$ and $\mathbf{x}^{(1)}$ are initialized such that $\sin\theta^{(1)} = 1/\sqrt{2-w}$. Then (20) implies that $\sin\theta^{(k)} = 1/\sqrt{2-w}$ for all $k \geq 1$. \square

Remark 5.1. *In addition, we can also specify the r -linear convergence factor. Since $\|\tilde{\mathbf{x}}^{(k)}\|/\|\tilde{\mathbf{x}}^{(k-1)}\| = w\|\tilde{\mathbf{y}}^{(k)}\|/\|\tilde{\mathbf{x}}^{(k-1)}\| = w \sin\theta^{(k)}$, it follows by similar arguments that the r -linear convergence factor is $w\sqrt{\sin\theta^{(1)}\sin\theta^{(2)}}$, which is bounded above by $w_0 = w/\sqrt{2-w}$ with the upper bound achieved when $\sin\theta^{(k)} = 1/\sqrt{2-w}$ for all $k \geq 1$, i.e., the setting described above such that (4) is an equality.*

5.3 Proof of Proposition 3

Proof. Following Theorem 1, we only need to consider the case $\lambda_{\max}(\mathbf{W}) = -\lambda_{\min}(\mathbf{W})$ and $m \geq 2$. We first claim that under this setting,

$$\|\tilde{\mathbf{x}}^{(k+2)}\| < \|\mathbf{W}\|^3 \|\tilde{\mathbf{x}}^{(k-1)}\| \quad (21)$$

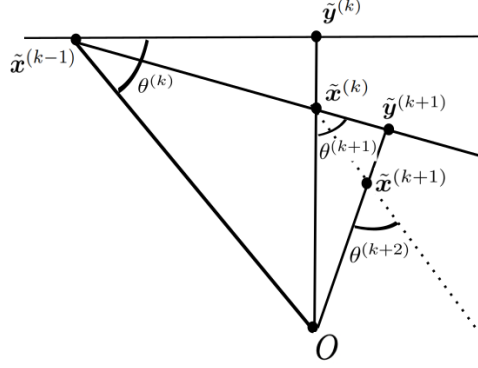


Figure 13: A visualization of AA(1) when \mathbf{W} is a scalar matrix.

for all $k \geq 1$. We prove (21) by contradiction. First, we note since $\|\tilde{\mathbf{x}}^{(k-1)}\| \geq \|\tilde{\mathbf{y}}^{(k)}\|$ and $\tilde{\mathbf{x}}^{(k)} = \mathbf{W}\tilde{\mathbf{y}}^{(k)}$,

$$\|\tilde{\mathbf{x}}^{(k)}\| = \|\mathbf{W}\tilde{\mathbf{y}}^{(k)}\| \leq \|\mathbf{W}\| \|\tilde{\mathbf{y}}^{(k)}\| \leq \|\mathbf{W}\| \|\tilde{\mathbf{x}}^{(k-1)}\| \quad (22)$$

with equality only achieved when $\tilde{\mathbf{y}}^{(k)} = \tilde{\mathbf{x}}^{(k-1)}$ and $\|\mathbf{W}\tilde{\mathbf{y}}^{(k)}\| = \|\mathbf{W}\| \|\tilde{\mathbf{y}}^{(k)}\|$. Assume

$$\|\tilde{\mathbf{x}}^{(k+2)}\| = \|\mathbf{W}\|^3 \|\tilde{\mathbf{x}}^{(k-1)}\|. \quad (23)$$

Then, following the analysis of (22) above, (23) holds only when for $i = 0, 1, 2$,

$$\tilde{\mathbf{y}}^{(k+i)} = \tilde{\mathbf{x}}^{(k-1+i)}, \quad \|\mathbf{W}\tilde{\mathbf{y}}^{(k+i)}\| = \|\mathbf{W}\| \|\tilde{\mathbf{y}}^{(k+i)}\|.$$

Since $\|\mathbf{W}\tilde{\mathbf{y}}^{(k)}\| = \|\mathbf{W}\| \|\tilde{\mathbf{y}}^{(k)}\|$, $\tilde{\mathbf{y}}^{(k)}$ lies in the span of the eigenvectors of \mathbf{W} with eigenvalues $\pm\|\mathbf{W}\|$. Let $\tilde{\mathbf{y}}^{(k)} = x_1\mathbf{v}_1 + x_2\mathbf{v}_2$, where \mathbf{v}_1 and \mathbf{v}_2 are eigenvectors of \mathbf{W} with eigenvalues $\|\mathbf{W}\|$ and $-\|\mathbf{W}\|$ respectively. Then $\tilde{\mathbf{x}}^{(k-1)} = \tilde{\mathbf{y}}^{(k)} = x_1\mathbf{v}_1 + x_2\mathbf{v}_2$, $\tilde{\mathbf{x}}^{(k)} = \mathbf{W}\tilde{\mathbf{y}}^{(k)} = \|\mathbf{W}\|(x_1\mathbf{v}_1 - x_2\mathbf{v}_2)$, and $\tilde{\mathbf{x}}^{(k+1)} = \|\mathbf{W}\|^2(x_1\mathbf{v}_1 + x_2\mathbf{v}_2)$. Let L_0 be the subspace containing $\tilde{\mathbf{x}}^{(k+1)}$, $\tilde{\mathbf{x}}^{(k)}$, $\tilde{\mathbf{x}}^{(k-1)}$, \dots , $\tilde{\mathbf{x}}^{(k-m_k+1)}$, then L_0 contains the line connecting $\tilde{\mathbf{x}}^{(k-1)}$ and $\tilde{\mathbf{x}}^{(k+1)} = \|\mathbf{W}\|^2\tilde{\mathbf{x}}^{(k-1)}$, so L_0 contains the origin. Recall that $\tilde{\mathbf{y}}^{(k+2)}$ is the point on L_0 with the smallest norm, so we must have $\tilde{\mathbf{y}}^{(k+2)} = \mathbf{0}$, which means that $\tilde{\mathbf{x}}^{(k+2)} = \mathbf{W}\tilde{\mathbf{y}}^{(k+2)} = \mathbf{0}$, violating our assumption in (23), and as a result (21) must hold.

Next, we prove there exists $c < 1$ such that

$$\|\tilde{\mathbf{x}}^{(k+2)}\| \leq c\|\mathbf{W}\|^3\|\tilde{\mathbf{x}}^{(k-1)}\| \quad (24)$$

for all $k \geq 1$ via contradiction. Following the argument of (22), we have

$$\max\left(\frac{\|\tilde{\mathbf{y}}^{(k)}\|}{\|\tilde{\mathbf{x}}^{(k-1)}\|}, \frac{\|\tilde{\mathbf{x}}^{(k)}\|}{\|\mathbf{W}\|\|\tilde{\mathbf{y}}^{(k)}\|}, \frac{\|\tilde{\mathbf{y}}^{(k+1)}\|}{\|\tilde{\mathbf{x}}^{(k)}\|}, \frac{\|\tilde{\mathbf{x}}^{(k+1)}\|}{\|\mathbf{W}\|\|\tilde{\mathbf{y}}^{(k+1)}\|}, \frac{\|\tilde{\mathbf{y}}^{(k+2)}\|}{\|\tilde{\mathbf{x}}^{(k+1)}\|}, \frac{\|\tilde{\mathbf{x}}^{(k+2)}\|}{\|\mathbf{W}\|\|\tilde{\mathbf{y}}^{(k+2)}\|}\right) \leq 1. \quad (25)$$

If (24) does not hold for all iterations, then given any $c \in (0, 1)$ there is an index k such that the product of the six terms in the left-hand side of (25) is larger than c , and as a result,

$$\min \left(\frac{\|\tilde{\mathbf{y}}^{(k)}\|}{\|\tilde{\mathbf{x}}^{(k-1)}\|}, \frac{\|\tilde{\mathbf{x}}^{(k)}\|}{\|\mathbf{W}\|\|\tilde{\mathbf{y}}^{(k)}\|}, \frac{\|\tilde{\mathbf{y}}^{(k+1)}\|}{\|\tilde{\mathbf{x}}^{(k)}\|}, \frac{\|\tilde{\mathbf{x}}^{(k+1)}\|}{\|\mathbf{W}\|\|\tilde{\mathbf{y}}^{(k+1)}\|}, \frac{\|\tilde{\mathbf{y}}^{(k+2)}\|}{\|\tilde{\mathbf{x}}^{(k+1)}\|}, \frac{\|\tilde{\mathbf{x}}^{(k+2)}\|}{\|\mathbf{W}\|\|\tilde{\mathbf{y}}^{(k+2)}\|} \right) > c. \quad (26)$$

Thus, for $i = 0, 1, 2$,

$$\|\tilde{\mathbf{y}}^{(k+i)}\| > c\|\tilde{\mathbf{x}}^{(k-1+i)}\|, \quad \|\mathbf{W}\tilde{\mathbf{y}}^{(k+i)}\| > c\|\mathbf{W}\|\|\tilde{\mathbf{y}}^{(k+i)}\|. \quad (27)$$

Recall $\tilde{\mathbf{x}}^{(k-1+i)} - \tilde{\mathbf{y}}^{(k+i)} \perp \tilde{\mathbf{y}}^{(k+i)}$. Then by the Pythagorean Theorem and the first inequality in (27) we see

$$\frac{\|\tilde{\mathbf{x}}^{(k-1+i)} - \tilde{\mathbf{y}}^{(k+i)}\|}{\|\tilde{\mathbf{y}}^{(k+i)}\|} < \frac{\sqrt{1-c^2}}{c}, \quad (28)$$

which implies $\tilde{\mathbf{x}}^{(k-1+i)}$ is close to $\tilde{\mathbf{y}}^{(k+i)}$ in a relative sense. Further, we note the right-hand side of the inequality approaches zero as c approaches 1. The second inequality in (27) implies that when c is chosen to be close to 1, $\tilde{\mathbf{y}}^{(k+i)}$ approximately lies in the span of the eigenvectors of \mathbf{W} with eigenvalues $\pm\|\mathbf{W}\|$. In particular, let L_1 and L_2 be the eigenspaces of \mathbf{W} with eigenvalues $\pm\|\mathbf{W}\|$, $P_{L_1 \oplus L_2}(\mathbf{x})$ denote the projection of the vector \mathbf{x} onto the direct sum of L_1 and L_2 , $\{\lambda_i(\mathbf{W})\}_{i=1}^n$ be the eigenvalues of \mathbf{W} , and $\beta = \max_{i:\lambda_i(\mathbf{W}) \neq \pm\|\mathbf{W}\|} |\lambda_i(\mathbf{W})|/\|\mathbf{W}\|$, then $0 \leq \beta < 1$ and the second inequality in (27) implies

$$\|P_{L_1 \oplus L_2} \tilde{\mathbf{y}}^{(k+i)}\|^2 + \beta^2 \|\tilde{\mathbf{y}}^{(k+i)} - P_{L_1 \oplus L_2} \tilde{\mathbf{y}}^{(k+i)}\|^2 > c^2 \|\tilde{\mathbf{y}}^{(k+i)}\|^2$$

from which we derive

$$\|\tilde{\mathbf{y}}^{(k+i)} - P_{L_1 \oplus L_2} \tilde{\mathbf{y}}^{(k+i)}\|^2 < \frac{1-c^2}{1-\beta^2} \|\tilde{\mathbf{y}}^{(k+i)}\|^2. \quad (29)$$

To obtain these inequalities we rewrite $\tilde{\mathbf{y}}^{(k+i)}$ using the eigenvectors of \mathbf{W} and make use of the fact $\|\mathbf{a}\|^2 = \|\mathbf{a}_1\|^2 + \|\mathbf{a}_2\|^2$ when $\mathbf{a} = \mathbf{a}_1 + \mathbf{a}_2$ and $\mathbf{a}_1 \perp \mathbf{a}_2$. Thus, (29) shows $\tilde{\mathbf{y}}^{(k+i)}$ approximately lies in the span of the eigenvectors of \mathbf{W} with eigenvalues $\pm\|\mathbf{W}\|$ and the right-hand side of (29) goes to zero as c approaches 1.

Following an argument similar to the proof of (21), we are able to show that when c is sufficiently close to 1, $\|\tilde{\mathbf{x}}^{(k+1)} - \|\mathbf{W}\|^2 \tilde{\mathbf{x}}^{(k-1)}\|/\|\tilde{\mathbf{x}}^{(k+1)}\| \approx 0$, which means $\|\tilde{\mathbf{y}}^{(k+2)}\|/\|\tilde{\mathbf{x}}^{(k+1)}\| \approx 0$, and it is a contradiction to the assumption (24) does not hold for any $0 < c < 1$, which in turn proves (24).

We prove the second half of the proposition with an example. Let $|w| < 1$, $\mathbf{W} := \text{Diag}(w, -w)$, $\mathbf{a} := \mathbf{0}$, $\tilde{\mathbf{x}}^{(0)} = [u, v]$ such that $(1-w)u^2 = (1+w)v^2$. Then AA(1) applied to this problem generates the sequences $\tilde{\mathbf{y}}^{(k)} = \tilde{\mathbf{x}}^{(k-1)}$ and $\tilde{\mathbf{x}}^{(k)} = \mathbf{W}\tilde{\mathbf{y}}^{(k)}$ for all $k \geq 2$. Therefore, AA(1) is reduced to the fixed-point method and it converges r -linearly with rate $\|\mathbf{W}\|$. \square

5.4 Proof of Theorem 4

Proof. The argument is similar to the proof of Theorem 1. Assuming $\mathbf{x}_* = 0$, let

$$\tilde{\mathbf{x}}^{(k)} := \mathbf{q}(\mathbf{x}^{(k)}) - \mathbf{x}^{(k)}, \quad \tilde{\mathbf{y}}^{(k+1)} := \sum_{j=k-m_k}^k \alpha_j^{(k)} \tilde{\mathbf{x}}^{(j)} = \sum_{j=k-m_k}^k \alpha_j^{(k)} (\mathbf{q}(\mathbf{x}^{(j)}) - \mathbf{x}^{(j)}),$$

and

$$\tilde{\mathbf{x}}^{(k+1)} := (\mathbf{q} - \mathbf{I})\mathbf{x}^{(k+1)} = (\mathbf{q} - \mathbf{I}) \left(\sum_{j=k-m_k}^k \alpha_j^{(k)} \mathbf{q}(\mathbf{q} - \mathbf{I})^{-1}(\tilde{\mathbf{x}}^{(j)}) \right). \quad (30)$$

We now prove the following properties:

$$(P1) \quad \|\tilde{\mathbf{y}}^{(k+1)}\| \leq \|\tilde{\mathbf{x}}^{(k)}\| \text{ with } \angle(O\tilde{\mathbf{y}}^{(k+1)}\tilde{\mathbf{x}}^{(k)}) \geq \pi/2$$

$$(P2) \quad \|\tilde{\mathbf{x}}^{(k+1)}\| \leq \|\mathbf{W}\| \|\tilde{\mathbf{y}}^{(k+1)}\| + \left(\max_{k-m_k \leq j \leq k} \|\tilde{\mathbf{x}}^{(j)}\|^2 \right) C_1^2.$$

The first property follows from the definition of $\tilde{\mathbf{y}}^{(k+1)}$, assuming $C_0 \geq 1$. Note, $\angle(O\tilde{\mathbf{y}}^{(k+1)}\tilde{\mathbf{x}}^{(k)}) \geq \pi/2$ instead of $\pi/2$ by the boundedness of the $\alpha_j^{(k)}$. The second property is proved using (30). Since $\mathbf{q}(\mathbf{x})$ is locally approximated by its first-order expansion at \mathbf{x}_* with an error on the order of $\|\mathbf{x} - \mathbf{x}_*\|^2$ and the $\alpha_j^{(k)}$'s are bounded, the second point is proved. To be more precise, from (30) and the facts $(\mathbf{q} - \mathbf{I})(\mathbf{x}) = (\mathbf{W} - \mathbf{I})\mathbf{x} + O(\|\mathbf{x}\|^2)$ and $(\mathbf{q} - \mathbf{I})^{-1}(\mathbf{x}) = (\mathbf{W} - \mathbf{I})^{-1}\mathbf{x} + O(\|\mathbf{x}\|^2)$ we see,

$$\begin{aligned} \tilde{\mathbf{x}}^{(k+1)} &= (\mathbf{q} - \mathbf{I}) \left(\sum_{j=k-m_k}^k \alpha_j^{(k)} \mathbf{q}[(\mathbf{q} - \mathbf{I})^{-1}(\tilde{\mathbf{x}}^{(j)})] \right) \\ &= (\mathbf{q} - \mathbf{I}) \left(\sum_{j=k-m_k}^k \alpha_j^{(k)} \left[\mathbf{W}(\mathbf{q} - \mathbf{I})^{-1}(\tilde{\mathbf{x}}^{(j)}) + \mathcal{O}(\|\tilde{\mathbf{x}}^{(j)}\|^2) \right] \right) \\ &= (\mathbf{q} - \mathbf{I}) \left(\sum_{j=k-m_k}^k \alpha_j^{(k)} \left[\mathbf{W}(\mathbf{W} - \mathbf{I})^{-1}(\tilde{\mathbf{x}}^{(j)}) + \mathcal{O}(\|\tilde{\mathbf{x}}^{(j)}\|^2) \right] \right) \\ &= (\mathbf{W} - \mathbf{I}) \left(\sum_{j=k-m_k}^k \alpha_j^{(k)} \left[\mathbf{W}(\mathbf{W} - \mathbf{I})^{-1}(\tilde{\mathbf{x}}^{(j)}) + \mathcal{O}(\|\tilde{\mathbf{x}}^{(j)}\|^2) \right] \right) \\ &\quad + \mathcal{O} \left(\left\| \sum_{j=k-m_k}^k \alpha_j^{(k)} \left[\mathbf{W}(\mathbf{W} - \mathbf{I})^{-1}(\tilde{\mathbf{x}}^{(j)}) + \mathcal{O}(\|\tilde{\mathbf{x}}^{(j)}\|^2) \right] \right\|^2 \right) \end{aligned}$$

where each equality was obtained via the local approximation of \mathbf{q} about \mathbf{x}_* . Then using the assumption that $\sum_{j=k-m_k}^k |\alpha_j^{(k)}|$ is bounded and applying linearity we see

$$\begin{aligned}
\tilde{\mathbf{x}}^{(k+1)} &= (\mathbf{W} - \mathbf{I}) \left(\sum_{j=k-m_k}^k \alpha_j^{(k)} \left[\mathbf{W}(\mathbf{W} - \mathbf{I})^{-1}(\tilde{\mathbf{x}}^{(j)}) + \mathcal{O}(\|\tilde{\mathbf{x}}^{(j)}\|^2) \right] \right) \\
&\quad + \mathcal{O} \left(\max_{k-m_k \leq i \leq k} \|\tilde{\mathbf{x}}^{(j)}\| \sum_{j=k-m_k}^k |\alpha_j^{(k)}| \right)^2 \\
&= (\mathbf{W} - \mathbf{I}) \left(\sum_{j=k-m_k}^k \alpha_j^{(k)} \left[\mathbf{W}(\mathbf{W} - \mathbf{I})^{-1}(\tilde{\mathbf{x}}^{(j)}) \right] \right) + \mathcal{O} \left(\max_{k-m_k \leq i \leq k} \|\tilde{\mathbf{x}}^{(j)}\| \right)^2 \\
&= \mathbf{W} \left(\sum_{j=k-m_k}^k \alpha_j^{(k)} \tilde{\mathbf{x}}^{(j)} \right) + \mathcal{O} \left(\max_{k-m_k \leq i \leq k} \|\tilde{\mathbf{x}}^{(j)}\| \right)^2 \\
&= \mathbf{W} \tilde{\mathbf{y}}^{(k+1)} + \mathcal{O} \left(\max_{k-m_k \leq i \leq k} \|\tilde{\mathbf{x}}^{(j)}\| \right)^2, \tag{31}
\end{aligned}$$

where the last equality came from the definition of $\tilde{\mathbf{y}}^{(k+1)}$. Thus, under mild assumptions there exists a constant $C_1 \geq 0$ such that

$$\|\tilde{\mathbf{x}}^{(k+1)} - \mathbf{W} \tilde{\mathbf{y}}^{(k+1)}\| \leq \left(\max_{k-m_k \leq j \leq k} \|\tilde{\mathbf{x}}^{(j)}\|^2 \right) C_1^2 \tag{32}$$

and (P2) is proved:

$$\|\tilde{\mathbf{x}}^{(k+1)}\| \leq \|\mathbf{W}\| \|\tilde{\mathbf{y}}^{(k+1)}\| + \left(\max_{k-m_k \leq j \leq k} \|\tilde{\mathbf{x}}^{(j)}\|^2 \right) C_1^2$$

for all points $\tilde{\mathbf{x}}^{(k)}$ near \mathbf{x}_* . Note, an assumption upon the continuity of the second-order derivatives of \mathbf{q} is sufficient to ensure the existence of C_1 .

We now prove AA(m) converges when the initialization is sufficiently close to \mathbf{x}_* . Define the sequence $d^{(k)}$ by $d^{(1)} = \|\tilde{\mathbf{x}}^{(1)}\|$ and $d^{(k+1)} = \|\mathbf{W}\| d^{(k)} + (\max_{k-m_k \leq j \leq k} d^{(k)})^2 C_1^2$ for $k \geq 1$. Observe, following (P1) and (P2) we have

$$\|\tilde{\mathbf{x}}^{(k+1)}\| \leq \|\mathbf{W}\| \|\tilde{\mathbf{x}}^{(k)}\| + \left(\max_{k-m_k \leq j \leq k} \|\tilde{\mathbf{x}}^{(j)}\|^2 \right) C_1^2. \tag{33}$$

Hence, by the definition of $d^{(k)}$, we see $\|\tilde{\mathbf{x}}^{(k)}\| \leq d^{(k)}$ for all k . Furthermore, from the definition of $d^{(k)}$ the sequence must converge to zero provided $d^{(1)}$ is small enough. As $d^{(1)}$ being small is synonymous with initializing the algorithm near \mathbf{x}_* , we have the convergence of AA(m).

Next, we prove the r -linear convergence factor of $\tilde{\mathbf{x}}^{(k)}$ is at least $\sqrt{w_0 \|\mathbf{W}\|}$. To accomplish this, it is sufficient to demonstrate there exists a sufficiently large K_0 such that for any $k > K_0$, there exists some $k_0 \leq k$ such that

$$\frac{\|\tilde{\mathbf{x}}^{(k+1)}\|}{\|\tilde{\mathbf{x}}^{(k_0)}\|} \leq (w_0 \|\mathbf{W}\|)^{(k+1-k_0)/2}. \tag{34}$$

We deal with (34) in cases. In particular, we let $m'_k = \max(m_k, m_{k-1} + 1)$.

Case 1: Assume $\max_{k-m'_k \leq j \leq k} \|\tilde{\mathbf{x}}^{(j)}\| \geq (w_0 \|\mathbf{W}\|)^{-(m'_k+1)/2} \|\tilde{\mathbf{x}}^{(k+1)}\|$. Then, (34) holds immediately with $k_0 = \arg \max_{k-m'_k \leq j \leq k} \|\tilde{\mathbf{x}}^{(j)}\|$.

Case 2: Assume $\max_{k-m'_k \leq j \leq k} \|\tilde{\mathbf{x}}^{(j)}\| \leq (w_0 \|\mathbf{W}\|)^{-(m'_k+1)/2} \|\tilde{\mathbf{x}}^{(k+1)}\|$. For large enough k , m_k becomes a constant; therefore, $(w_0 \|\mathbf{W}\|)^{-(m_k+1)/2} = O(1)$ and combining (P2) with our assumption for this case we have

$$\|\tilde{\mathbf{x}}^{(k+1)}\| \leq \|\mathbf{W}\| \|\tilde{\mathbf{y}}^{(k+1)}\| + O\left(\max_{k-m_k \leq j \leq k} \|\tilde{\mathbf{x}}^{(j)}\|^2\right) \leq \|\mathbf{W}\| \|\tilde{\mathbf{y}}^{(k+1)}\| + O(\|\tilde{\mathbf{x}}^{(k+1)}\|^2). \quad (35)$$

Having proved the convergence of AA(m), we know $\|\tilde{\mathbf{x}}^{(k)}\|$ converges to zero, so for large k $\|\tilde{\mathbf{x}}^{(k+1)}\| \leq \|\tilde{\mathbf{y}}^{(k+1)}\|$. Combining this with $\|\tilde{\mathbf{y}}^{(k+1)}\| \leq \|\tilde{\mathbf{x}}^{(k)}\|$ in (P1), the assumption in case 2 implies

$$\max_{k-m'_k \leq j \leq k} \|\tilde{\mathbf{x}}^{(j)}\| \leq (w_0 \|\mathbf{W}\|)^{-(m'_k+1)/2} \|\tilde{\mathbf{x}}^{(k)}\|.$$

Apply the same argument as in (35),

$$\|\tilde{\mathbf{x}}^{(k)}\| \leq \|\mathbf{W}\| \|\tilde{\mathbf{y}}^{(k)}\| + O(\|\tilde{\mathbf{x}}^{(k)}\|^2). \quad (36)$$

Having proved the convergence of AA(m), we know $\|\tilde{\mathbf{x}}^{(k)}\|$ converges to zero, so for large k

$$O(\|\tilde{\mathbf{x}}^{(k)}\|^2) = o(\|\tilde{\mathbf{x}}^{(k)}\|), \quad \|\tilde{\mathbf{x}}^{(k)}\| \leq \|\mathbf{W}\| \|\tilde{\mathbf{y}}^{(k)}\| + o(\|\tilde{\mathbf{x}}^{(k)}\|). \quad (37)$$

Let $\hat{\mathbf{y}}^{(k+1)}$ be the projection of the origin onto the line connecting $\tilde{\mathbf{x}}^{(k-1)}$ and $\tilde{\mathbf{x}}^{(k)}$. Now, (36) implies $\|\tilde{\mathbf{x}}^{(k)}\| \leq \|\mathbf{W}\| \|\tilde{\mathbf{y}}^{(k)}\| + O(\|\tilde{\mathbf{x}}^{(k)}\|^2) \leq \|\mathbf{W}\| \|\tilde{\mathbf{y}}^{(k)}\| + \frac{1}{2} \|\tilde{\mathbf{x}}^{(k)}\|$ for large k , so $\|\tilde{\mathbf{x}}^{(k)}\| \leq 2\|\mathbf{W}\| \|\tilde{\mathbf{y}}^{(k)}\| \leq 2\|\tilde{\mathbf{y}}^{(k)}\|$. Thus, for large k it follows

$$\begin{aligned} \|\tilde{\mathbf{x}}^{(k)} - \hat{\mathbf{y}}^{(k+1)}\| &\leq \|\tilde{\mathbf{x}}^{(k)}\| + \|\hat{\mathbf{y}}^{(k+1)}\| \\ &\leq 2\|\tilde{\mathbf{x}}^{(k)}\| \\ &\leq 2\|\tilde{\mathbf{y}}^{(k)}\| + O(\|\tilde{\mathbf{x}}^{(k)}\|^2) \\ &\leq 2\|\tilde{\mathbf{y}}^{(k)}\| + O(\|\tilde{\mathbf{y}}^{(k)}\|^2). \end{aligned} \quad (38)$$

From (P1) we have $\|\tilde{\mathbf{x}}^{(k-1)}\| \geq \|\tilde{\mathbf{y}}^{(k)}\|$, so

$$\|\tilde{\mathbf{x}}^{(k)} - \tilde{\mathbf{x}}^{(k-1)}\| \geq \|\tilde{\mathbf{x}}^{(k-1)}\| - \|\tilde{\mathbf{x}}^{(k)}\| \geq (1 - \|\mathbf{W}\|) \|\tilde{\mathbf{y}}^{(k)}\| - O(\|\tilde{\mathbf{y}}^{(k)}\|^2) \quad (39)$$

which follows by (P1), (P2), and our initial assumption. Combining (38) and (39) we have

$$\hat{\mathbf{y}}^{(k+1)} - \tilde{\mathbf{x}}^{(k)} = c(\tilde{\mathbf{x}}^{(k)} - \tilde{\mathbf{x}}^{(k-1)})$$

with

$$|c| \leq \frac{2\|\tilde{\mathbf{y}}^{(k)}\| + O(\|\tilde{\mathbf{y}}^{(k)}\|^2)}{(1 - \|\mathbf{W}\|) \|\tilde{\mathbf{y}}^{(k)}\| - O(\|\tilde{\mathbf{y}}^{(k)}\|^2)} = \frac{2}{1 - \|\mathbf{W}\|} + o(1),$$

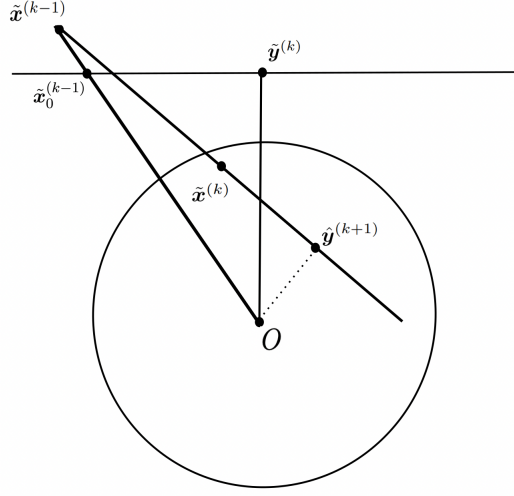


Figure 14: A visualization of the proof of nonlinear operators.

as visualized in Figure 14. As a result, when C_0 is large enough, i.e., $C_0 > \frac{2}{1-\|\mathbf{W}\|} + 1 + o(1)$, we have

$$\|\tilde{\mathbf{y}}^{(k+1)}\| \leq \|\hat{\mathbf{y}}^{(k+1)}\| \leq (w_0 + o(1))\|\tilde{\mathbf{x}}^{(k-1)}\|, \quad (40)$$

where the second inequality follows the argument in Theorem 1. We note that the $o(1)$ factor follows from combining (32) with the argument in (36), which implies that

$$\|\tilde{\mathbf{x}}^{(k)} - \mathbf{W}\tilde{\mathbf{y}}^{(k)}\| \leq o(\|\tilde{\mathbf{x}}^{(k)}\|)$$

and $\tilde{\mathbf{x}}^{(k)}$ lie in the sphere with the same center as in Theorem 1 but with radius larger by a factor of $1 + o(1)$. Another technical issue regarding the adaptation of the proof of Theorem 1 is as follows: (P1) implies $\angle(O\tilde{\mathbf{y}}^{(k)}\tilde{\mathbf{x}}^{(k-1)}) \geq \pi/2$ while the proof of Theorem 1 depends on a more restrictive condition of $\angle(O\tilde{\mathbf{y}}^{(k)}\tilde{\mathbf{x}}^{(k-1)}) = \pi/2$. We refer the readers to the visualizations in Figure 11 and Figure 14 for a comparison. Despite the different assumption, the proof of Theorem 1 remains applicable here, supported by the following argument. The proof relies on estimating the upper bound of $\angle(O\tilde{\mathbf{x}}^{(k-1)}\tilde{\mathbf{x}}^{(k)})$, but $\angle(O\tilde{\mathbf{x}}^{(k-1)}\tilde{\mathbf{x}}^{(k)})$ is maximized when $\angle(O\tilde{\mathbf{y}}^{(k)}\tilde{\mathbf{x}}^{(k-1)}) = \pi/2$, i.e., when the more restrictive assumption in the proof of Theorem 1 holds. This fact is evident by the visualization in Figure 14, where $\angle(O\tilde{\mathbf{x}}^{(k-1)}\tilde{\mathbf{x}}^{(k)}) \leq \angle(O\tilde{\mathbf{x}}_0^{(k-1)}\tilde{\mathbf{x}}^{(k)})$, and $\angle(O\tilde{\mathbf{y}}^{(k)}\tilde{\mathbf{x}}_0^{(k-1)}) = \pi/2$. As a result, the argument in Theorem 1 applies, despite the difference in the assumption on $\angle(O\tilde{\mathbf{y}}^{(k)}\tilde{\mathbf{x}}_0^{(k-1)})$. Thus, combining (40) with (35) and (37), we have

$$\frac{\|\tilde{\mathbf{x}}^{(k+1)}\|}{\|\tilde{\mathbf{x}}^{(k-1)}\|} \leq w_0\|\mathbf{W}\| + o(\|\tilde{\mathbf{x}}^{(k+1)}\|), \quad (41)$$

which implies (34) for sufficiently large $k_0 = k - 1$. \square

6 Conclusion

This paper studies the convergence properties of the classical windowed AA algorithm and provides the first argument showing it improves the root-linear convergence factor of the fixed-point iteration when \mathbf{q} is linear and symmetric. We extend our investigation to nonlinear operators \mathbf{q} possessing a symmetric Jacobian at fixed points and prove an adapted version of the method locally enjoys improved root-linear convergence. Our theoretical discoveries were validated through simulations where we showcased AA(m) significantly outperforms the fixed-point iteration for TME. In the future, we hope to generalize our results to non-symmetric linear operators and refine the estimations of the r -linear convergence factor.

Acknowledgements

First, GL thanks Yousef Saad for introducing him to Anderson acceleration. The authors also thank and acknowledge their funding sources as this material is based upon work supported by the National Science Foundation Graduate Research Fellowship Program under Grant No. 2237827, NSF Award DMS-2152766, and NSF DMS-2318926. Any opinions, findings, and conclusions or recommendations expressed in this material are those of the author(s) and do not necessarily reflect the views of the National Science Foundation.

References

- Anderson, D. G. (1965), *Iterative procedures for nonlinear integral equations*, J. ACM, 12(4), pp. 547–560, doi.org/10.1145/321296.321305.
- Bertrand, Q. and Massias, M. (2021), *Anderson acceleration of coordinate descent*, in Proceedings of the 24th Int. Conf. on Artificial Intelligence and Statistics, PMLR 130, pp. 1288–1296.
- Bian, W. and Chen, X. (2022), *Anderson acceleration for nonsmooth fixed point problems*, SIAM J. Numer. Anal., 60(5), pp. 2565–2591, doi.org/10.1137/22M1475983.
- Bian, W., Chen, X., and Kelley, C.T. (2021), *Anderson acceleration for a class of nonsmooth fixed-point problems*, SIAM J. Sci. Comput., 43(5), pp. 51–520, doi.org/10.1137/20M132938X.
- Both, J. W., Kumar, K., Nordbotten, J. M., and Radu, F. A. (2019), *Anderson accelerated fixed-stress splitting schemes for consolidation of unsaturated porous media*, Comput. Math. Appl., 77(6), pp. 1479–1502, doi.org/10.1016/j.camwa.2018.07.033.

- Brezinski, C., Cipolla, S., Redivo-Zaglia, M., and Saad, Y. (2022), *Shanks and Anderson-type acceleration techniques for systems of nonlinear equations*, IMA J. Numer. Anal., 42(4), pp. 3058–3093, doi.org/10.1093/imanum/drab061.
- Chen, Y., Wiesel, A., and Hero, A. O. (2011), *Robust shrinkage estimation of high-dimensional covariance matrices*, IEEE Trans. Signal Process., 59(9), pp. 4097–4107.
- De Sterck, H. and He, Y. (2022), *Linear asymptotic convergence of Anderson acceleration: fixed-point analysis*, SIAM J. Numer. Anal., 43(4), pp. 1755–1783, doi.org/10.1137/21M1449579.
- De Sterck, H., He, Y., and Krzysik, O.A. (2024), *Anderson acceleration as a Krylov method with application to convergence analysis*, J. Sci. Comput., 99(1), doi.org/10.1007/s10915-024-02464-x.
- De Sterck, H., Krzysik O. A., and Smith, A. (2024), *On the convergence of restarted Anderson acceleration for symmetric linear systems*, arXiv preprint arXiv:2312.04776.
- d’Aspremont, A., Scieur, D., and Taylor, A. (2021), *Acceleration Methods*, Found. Trends in Opt., 5(1-2), pp. 1-245, doi.org/10.1561/2400000036.
- Evans, C., Pollock, S., Rebholz, L. G., and Xiao, M. (2020), *A proof that Anderson acceleration improves the convergence rate in linearly converging fixed-point methods (but not in those converging quadratically)*, SIAM J. Numer. Anal., 58(1), pp. 788–810, doi.org/10.1137/19M1245384.
- Fang, H.-r. and Saad, Y. (2009), *Two classes of multisection methods for nonlinear acceleration*, Numer. Linear Algebra Appl., 16(3), pp. 197–221, doi.org/10.1002/nla.617.
- Frahm, G. and Jaekel, U. (2007). *Tyler’s M-estimator, random matrix theory, and generalized elliptical distributions with applications to finance*, Discussion Papers in Econometrics and Statistics, No. 2/07, University of Cologne, Institute of Econometrics and Statistics.
- Frahm, G. and Jaekel, U. (2010), *A generalization of Tyler’s M-estimators to the case of incomplete data*, Comput. Statist. Data Anal., 54(2), pp. 374–393, doi.org/10.1016/j.csda.2009.08.019.
- Franks, W. C. and Moitra, A. (2020), *Rigorous guarantees for Tyler’s M-estimator via quantum expansion*, in Proceedings of Thirty-Third Conference on Learning Theory, PMLR, 125, pp. 1601-1632.
- Geist, M. and Scherrer, B. (2018), *Anderson acceleration for reinforcement learning*, arXiv preprint arXiv:1809.09501.
- Goes, J., Lerman, G., and Nadler, B. (2020). *Robust sparse covariance estimation by thresholding Tyler’s M-estimator*, Ann. Statist., 48(1), pp. 86-100, doi.org/10.1214/18-AOS1793.

- Kelley, C. T. (2018), *Numerical methods for nonlinear equations*, Acta Numer., 27(1), pp. 207-287, doi.org/10.1017/S0962492917000113.
- Kent, J. T. and Tyler, D. E. (1988), *Maximum likelihood estimation for the wrapped Cauchy distribution*, J. Appl. Stat., 15(2), pp. 247–254, doi.org/10.1080/02664768800000029.
- Ollila, E. and Koivunen, V. (2003), *Robust antenna array processing using M-estimators of pseudo-covariance*, in Proceedings of the 14th IEEE Symposium on Personal, Indoor and Mobile Radio Communications (PIMRC), 3, pp. 2659–2663.
- Ollila, E. and Tyler, D. E. (2012), *Distribution-free detection under complex elliptically symmetric clutter distribution*, in Proceedings of the 7th IEEE Sensor Array and Multichannel Signal Processing Workshop, (SAM), pp. 413–416.
- Picard, É. (1890), *Memoire sur la theorie des equations aux derivees partielles et la methode des approximations successives*, Journal de Mathématiques pures et appliquées, 6, pp. 145-210.
- Pollock, S. and Rebholz, L. G. (2021), *Anderson acceleration for contractive and noncontractive operators*, IMA J. Numer. Anal., 41(4), pp. 2841-2872, doi.org/10.1093/imanum/draa095.
- Pollock, S., Rebholz, L. G., and Xiao, M. (2019), *Anderson-accelerated convergence of Picard iterations for incompressible Navier–Stokes equations*. SIAM J. Numer. Anal., 57(2), pp. 615-637, doi.org/10.1137/18M1206151.
- Potra, F. A. and Engler, H. (2013), *A characterization of the behavior of the Anderson acceleration on linear problems*, Linear Algebra Appl., 438(3), pp. 1002-1011, doi.org/10.1016/j.laa.2012.09.008.
- Pulay, P. (1980). *Convergence acceleration of iterative sequences. the case of scf iteration*, Chem. Phys. Lett., 73(2), pp. 393–398, [doi.org/10.1016/0009-2614\(80\)80396-4](https://doi.org/10.1016/0009-2614(80)80396-4).
- Rebholz, L. G. and Xiao, M. (2023), *The effect of Anderson acceleration on superlinear and sublinear convergence*, J. Sci. Comput., 96(2), doi.org/10.1007/s10915-023-02262-x.
- Scieur, D. (2019), *Generalized framework for nonlinear acceleration*. arXiv preprint arXiv:1903.08764.
- Scieur, D., d'Aspremont, A., and Bach, F. (2016), *Regularized nonlinear acceleration*, in Advances in Neural Information Processing Systems, 29. pp. 3-43.
- Shi, W., Song, S., Wu, H., Hsu, Y.-C., Wu, C., and Huang, G. (2019), *Regularized Anderson acceleration for off-policy deep reinforcement learning*, in Advances in Neural Information Processing Systems, 32.

- Sun, K., Wang, Y., Liu, Y., Pan, B., Jui, S., Jiang, B., Kong, L., et al. (2021), *Damped Anderson mixing for deep reinforcement learning: acceleration, convergence, and stabilization*, in Advances in Neural Information Processing Systems, 34, pp. 3732–3743.
- Toth, A. and Kelley, C. T. (2015), *Convergence analysis for Anderson acceleration*, SIAM J. Numer. Anal., 53(2), pp. 805–819, doi.org/10.1137/130919398.
- Tyler, D. E. (1987a), *A distribution-free M-estimator of multivariate scatter*, Ann. Statist., 15(1), pp. 234–251.
- Tyler, D. E. (1987b), *Statistical analysis for the angular central Gaussian distribution on the sphere*, Biometrika, 74(3), pp. 579–589.
- Walker, H. F. and Ni, P. (2011), *Anderson acceleration for fixed-point iterations*, SIAM J. Numer. Anal., 49(4), pp. 1715–1735, doi.org/10.1137/10078356X.
- Zhang, J., O’Donoghue, B., and Stephen B. (2020), *Globally convergent type-I Anderson acceleration for nonsmooth fixed-point iterations*, SIAM J. Optim., 30(4), pp. 3170–3197, doi.org/10.1137/18M1232772.
- Zhang, T., Cheng, X., and Singer, A. (2016), *Marčenko-Pastur law for Tyler’s M-estimator*, J. Multivar. Anal., 149, pp. 114–123, doi.org/10.1016/j.jmva.2016.03.010.